

**Satellite Earth Stations and Systems (SES);
Satellite Component of UMTS/IMT-2000;
Evaluation of the OFDM as a Satellite Radio Interface**



Reference

DTR/SES-00252

Keywords

satellite, UMTS

ETSI

650 Route des Lucioles
F-06921 Sophia Antipolis Cedex - FRANCE

Tel.: +33 4 92 94 42 00 Fax: +33 4 93 65 47 16

Siret N° 348 623 562 00017 - NAF 742 C
Association à but non lucratif enregistrée à la
Sous-Préfecture de Grasse (06) N° 7803/88

Important notice

Individual copies of the present document can be downloaded from:

<http://www.etsi.org>

The present document may be made available in more than one electronic version or in print. In any case of existing or perceived difference in contents between such versions, the reference version is the Portable Document Format (PDF). In case of dispute, the reference shall be the printing on ETSI printers of the PDF version kept on a specific network drive within ETSI Secretariat.

Users of the present document should be aware that the document may be subject to revision or change of status. Information on the current status of this and other ETSI documents is available at

<http://portal.etsi.org/tb/status/status.asp>

If you find errors in the present document, please send your comment to one of the following services:

http://portal.etsi.org/chaicor/ETSI_support.asp

Copyright Notification

No part may be reproduced except as authorized by written permission.
The copyright and the foregoing restriction extend to reproduction in all media.

© European Telecommunications Standards Institute 2008.
All rights reserved.

DECT™, PLUGTESTS™, UMTS™, TIPHON™, the TIPHON logo and the ETSI logo are Trade Marks of ETSI registered for the benefit of its Members.

3GPP™ is a Trade Mark of ETSI registered for the benefit of its Members and of the 3GPP Organizational Partners.

Contents

Intellectual Property Rights	5
Foreword.....	5
1 Scope	6
2 References	6
2.1 Normative references	6
2.2 Informative references.....	6
3 Definitions, symbols and abbreviations	7
3.1 Definitions.....	7
3.2 Symbols.....	8
3.3 Abbreviations	8
4 OFDM technology and background	9
4.1 OFDM Fundamentals	9
4.1.1 OFDM Definitions.....	9
4.1.2 OFDM Signal Generation.....	10
4.1.3 Guard Interval	11
4.1.4 Impact of Guard Interval.....	12
4.1.5 Impact of Symbol Duration	12
4.1.6 Impact of Inter-Carrier Spacing.....	12
4.1.7 OFDM Inactive Sub-Carriers.....	12
4.1.8 Time-Frequency Multiplexing.....	13
4.1.9 OFDM Signal Reception Using the FFT	14
4.2 OFDM for Mobile Terrestrial and Satellite Scenario	14
5 OFDM and the satellite environment	15
5.1 Non-Linearity Effects and Predistortion Techniques	15
5.1.1 Compensation Techniques	15
5.1.2 Digital Predistortion Techniques	16
5.1.3 Multi-Beam Coverage Using OFDM.....	16
6 OFDM feasibility	17
6.1 Physical Layer Structure in the OFDM Downlink	17
6.1.1 Physical Channel	17
6.1.1.1 OFDM Physical Channel Definition	18
6.1.2 Channel Coding and Multiplexing.....	19
6.1.3 Physical Channel Mapping	20
6.1.4 User Traffic Multiplexing Solutions.....	20
6.1.4.1 Solution based on a generic Costas sequence	20
6.2 Spectrum Compatibility	22
7 OFDM Evaluation Scenario	23
7.1 Reference System Scenario for OFDM S-DMB Analysis.....	23
7.2 Reference OFDM configurations for the evaluation	24
8 Simulation Results.....	25
8.1 Uncoded System Performance	25
8.1.1 AWGN Channel.....	25
8.1.2 Non-linear channel.....	26
8.2 WCDMA Coding Performance	27
8.2.1 Non selective Rice fading	29
8.2.2 Frequency Selective Channel.....	30
9 Link Budget Study	36
9.1 System parameters.....	36
9.1.1 Satellite parameters.....	36
9.1.2 UE parameters	36
9.1.3 Physical layer configuration and performances	36

9.2	Link budgets	37
9.2.1	Handset	37
9.2.2	Handheld.....	38
9.2.3	Vehicular	39
10	Conclusions	39
History	41

Intellectual Property Rights

IPRs essential or potentially essential to the present document may have been declared to ETSI. The information pertaining to these essential IPRs, if any, is publicly available for **ETSI members and non-members**, and can be found in ETSI SR 000 314: *"Intellectual Property Rights (IPRs); Essential, or potentially Essential, IPRs notified to ETSI in respect of ETSI standards"*, which is available from the ETSI Secretariat. Latest updates are available on the ETSI Web server (<http://webapp.etsi.org/IPR/home.asp>).

Pursuant to the ETSI IPR Policy, no investigation, including IPR searches, has been carried out by ETSI. No guarantee can be given as to the existence of other IPRs not referenced in ETSI SR 000 314 (or the updates on the ETSI Web server) which are, or may be, or may become, essential to the present document.

Foreword

This Technical Report (TR) has been produced by ETSI Technical Committee Satellite Earth Stations and Systems (SES).

1 Scope

The present document entails a feasibility study that evaluates the use of the OFDM Radio Interface proposed the 3GPP TR 25.892 [i.1] as Satellite Radio Interface on the satellite downlink, presenting physical layer results and link budget studies. The present document contains informative elements that should serve as a starting point for the definition and finalization of advanced Satellite Radio Interfaces. The adoption of the OFDM Radio Interface results in higher link margin under key propagation conditions such as the NLOS propagation case and when CGCs are considered.

2 References

References are either specific (identified by date of publication and/or edition number or version number) or non-specific.

- For a specific reference, subsequent revisions do not apply.
- Non-specific reference may be made only to a complete document or a part thereof and only in the following cases:
 - if it is accepted that it will be possible to use all future changes of the referenced document for the purposes of the referring document;
 - for informative references.

Referenced documents which are not found to be publicly available in the expected location might be found at <http://docbox.etsi.org/Reference>.

For online referenced documents, information sufficient to identify and locate the source shall be provided. Preferably, the primary source of the referenced document should be cited, in order to ensure traceability. Furthermore, the reference should, as far as possible, remain valid for the expected life of the document. The reference shall include the method of access to the referenced document and the full network address, with the same punctuation and use of upper case and lower case letters.

NOTE: While any hyperlinks included in this clause were valid at the time of publication ETSI cannot guarantee their long term validity.

2.1 Normative references

The following referenced documents are indispensable for the application of the present document. For dated references, only the edition cited applies. For non-specific references, the latest edition of the referenced document (including any amendments) applies.

Not applicable.

2.2 Informative references

The following referenced documents are not essential to the use of the present document but they assist the user with regard to a particular subject area. For non-specific references, the latest version of the referenced document (including any amendments) applies.

- [i.1] 3GPP TR 25.892 (V6.0.0): "3rd Generation Partnership Project; Technical Specification Group Radio Access Network; Feasibility Study for Orthogonal Frequency Division Multiplexing (OFDM) for UTRAN enhancement (Release 6)".
- [i.2] 3GPP TR 25.858 (V5.0.0): "3rd Generation Partnership Project; Technical Specification Group Radio Access Network; High Speed Downlink Packet Access: Physical Layer Aspects (Release 5)".

- [i.3] ETSI TS 125 212: "Universal Mobile Telecommunications System (UMTS); Multiplexing and channel coding (FDD) (3GPP TS 25.212 version 5.9.0 Release 5)".
- [i.4] S. Chang: "Compensation of nonlinear distortion in RF power amplifiers", Wiley Encyclopedia of Telecommunications, J.J. Proakis Ed., 2002.
- [i.5] S. Benedetto and E. Biglieri: "Nonlinear equalization of digital satellite channels", IEEE J. Select. Areas Comm., vol. 1, pp. 57-62, Jan. 1983.
- [i.6] J.K. Cavers: "Amplifier Linearization using a digital predistorter with fast adaptation and low memory requirements", IEEE Trans. Vehic. Tech., vol. 39, pp. 31-40, Nov. 1990.
- [i.7] P. Salmi, M. Neri, and G.E. Corazza: "Fractional Predistortion. Techniques with Robust Modulation Schemes for Fixed and mobile Broadcasting", 13th IST Mobile & Wireless Communications Summit (IST2004), pp. 990-995, June 2004.
- [i.8] S.W. Golomb, and H. Taylor: "Construction and Properties of Costas Array", Proc. IEEE, vol. 72, pp. 1143-1163, Sep. 1984.
- [i.9] S. Cioni, G.E. Corazza, M. Neri, and A. Vanelli-Coralli: "On the Use of OFDM Radio Interface for Satellite Digital Multimedia Broadcasting Systems", International Journal of Satellite Communications and Networking, February 2006, Int. J. Satell. Commun. Network. 2006; 24:153-167, published online in Wiley InterScience (www.interscience.wiley.com). DOI: 10.1002/sat.836.

3 Definitions, symbols and abbreviations

3.1 Definitions

For the purposes of the present document, the following terms and definitions apply:

cell: geographical area under Complementary Ground Component coverage

downlink: unidirectional radio link for the transmission of signals from a satellite to a UE

forward link: unidirectional radio link for the transmission of signals from a gateway to a UE via a satellite

guard interval / guard time: number of samples inserted between useful OFDM symbols, in order to combat inter-OFDM-symbol-interference induced by channel dispersion and to assist receiver synchronization

NOTE: It may also be used to aid spectral shaping. The guard interval may be divided into a prefix (inserted at the beginning of the useful OFDM symbol) and a postfix (inserted at the end of the previous OFDM symbol).

inter-carrier frequency / sub-carrier separation: frequency separation between OFDM sub-carriers, defined as the OFDM sampling frequency divided by the FFT size

OFDM unit: group of constellation symbols to be mapped onto a sub-band, a subset of the OFDM carriers

OFDM samples: discrete-time complex values generated at the output of the IFFT, which may be complemented by the insertion of additional complex values (such as samples for pre/post fix and time windowing)

NOTE: Additional digital signal processing (such as filtering) may be applied to the resulting samples, prior to being fed to a digital-to-analog converter.

OFDM sampling frequency: total number of samples, including guard interval samples, transmitted during one OFDM symbol interval, divided by the symbol period

repeater: device (e.g. CGC) that receives, amplifies and transmits the radiated or conducted RF carrier both in the down-link direction (from the satellite to the mobile area) and in the up-link direction (from the mobile to the satellite)

return link: unidirectional radio link for the transmission of signals from a UE to a gateway via a satellite

rice factor: power ratio between LOS component and diffuse component

spot: geographical area under beam coverage

uplink: unidirectional radio link for the transmission of signals from a UE to a satellite

useful OFDM symbol: time domain signal corresponding to the IFFT/FFT window, excluding the guard time

useful OFDM symbol duration: time duration of the useful OFDM symbol

3.2 Symbols

For the purposes of the present document, the following symbols apply:

F_0	OFDM sampling frequency
F_d	Maximum Doppler shift.
N	Total number of IFFT/FFT bins (sub-carriers)
N_p	Number of prefix samples
N_u	Number of modulated sub-carriers (i.e. sub-carriers carrying information)
T_s	OFDM symbol period
T_g	OFDM prefix duration
T_u	OFDM useful symbol duration
Δf	Sub-carrier separation

3.3 Abbreviations

For the purposes of the present document, the following abbreviations apply:

ACI	Adjacent Channel Interference
APSK	Amplitude and Phase Shift Keying
AWGN	Additive White Gaussian Noise
BER	Bit Error Rate
C/N	Carrier to Noise power ratio
CGC	Complementary Ground Component
CRC	Cyclic Redundancy Check
CPICH	Common Pilot Channel
DC-RF	Direct Current to Radio Frequency
DL	Down Link
EIRP	Effective Isotropic Radiated Power
FDM	Frequency Division Multiplexing
FFS	For Further Study
FFT	Fast Fourier Transform
FIR	Finite Impulse Response
GEO	Geostationary Earth Orbit
GW	GateWay
HARQ	Hybrid Automatic Repeat reQuest
HPA	High Power Amplifiers
HSDPA	High Speed Downlink Packet Access
HS-DSCH	High Speed - Downlink Shared CHannel
IBO	Input Back-Off
IFFT	Inverse Fast Fourier Transform
IMR	Intermediate Module Repeater
ISI	Inter Symbol Interference
LOS	Line-Of-Sight
LTWTA	Linearized Travelling Wave Tube Amplifier
LUT	Look-Up Table
MAC	Medium Access Control
MIMO	Multiple Input Multiple Output
NL	Non Linear
NLOS	No Line-Of-Sight
OBO	Output Back Off

OFDM	Orthogonal Frequency Division Multiplexing
PAPR	Peak-to-Average Power Ratio
PDSCH	Physical Downlink Shared CHannel
PER	Packet Error Rate
PhCh	Physical Channel
PSK	Phase Shift Keying
QAM	Quadrature Amplitude Modulation
SCCH	Shared Control CHannel
S-DMB	Satellite-Digital Mobile Broadcasting
SFN	Single Frequency Network
SNR	Signal-to-Noise Ratio
T-F	Time-Frequency
TPCCH	Transmit Power Control CHannel
TTI	Transmission Time Interval
TWTA	Travelling Wave Tube Amplifier
UE	User Equipment
UTRAN	UMTS Terrestrial Radio Access Network
WCDMA	Wideband Code Division Multiple Access

4 OFDM technology and background

4.1 OFDM Fundamentals

4.1.1 OFDM Definitions

The technique of Orthogonal Frequency Division Multiplexing (OFDM) is based on the well-known technique of Frequency Division Multiplexing (FDM). In FDM different streams of information are mapped onto separate parallel frequency channels. Each FDM channel is separated from the others by a frequency guard band to reduce interference between adjacent channels.

The OFDM technique differs from traditional FDM in the following interrelated ways:

- 1) multiple carrier multiple carriers (called sub-carriers) carry the information stream;
- 2) the sub-carriers are orthogonal to each other; and
- 3) a guard time may be added to each symbol to combat the channel delay spread and inter-symbol interference induced by linear distortion.

These concepts are illustrated in the time-frequency representation of OFDM presented in figure 1.

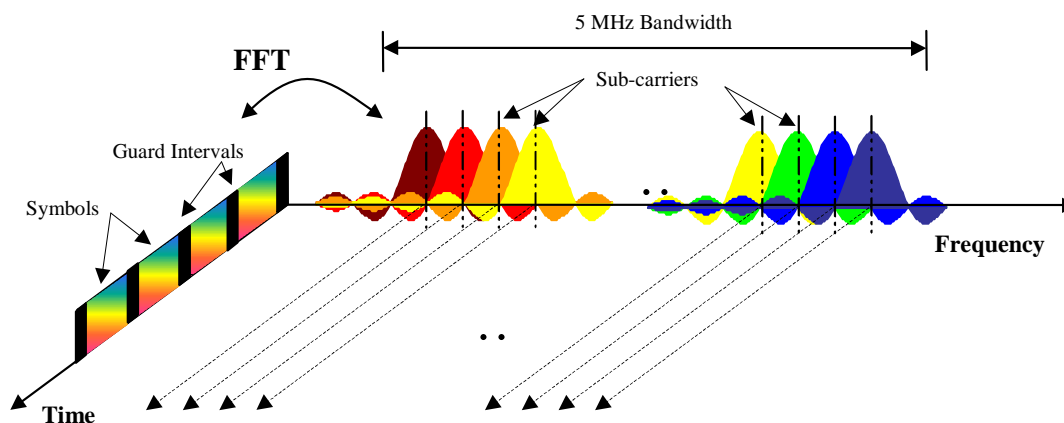


Figure 1: Frequency-Time representation of an OFDM Signal

Since the orthogonality is guaranteed between overlapping sub-carriers and between consecutive OFDM symbols in the presence of time/frequency dispersive channels the data symbol density in the time-frequency plane can be maximized.

4.1.2 OFDM Signal Generation

Data symbols are synchronously and independently transmitted over a high number of closely spaced orthogonal sub-carriers using linear modulation (either PSK, APSK or QAM). The generation of the QAM/OFDM signal can be conceptually illustrated as in figure 2, where ω_n is the n^{th} sub-carrier frequency (in rad/s) and $1/T_u$ is the QAM symbol rate. Note that the sub-carriers frequencies are equally spaced and hence the sub-carrier separation is constant. That is:

$$\frac{|\omega_n - \omega_{n-1}|}{2\pi} = \Delta f, \quad n \in [1, N - 1].$$

In practice, the OFDM signal can be generated using IFFT digital signal processing. The baseband representation of the OFDM signal generation using an N -point IFFT is illustrated in figure 3, where $a(mN+n)$ refers to the n^{th} sub-channel modulated data symbol, during the time period $mT_u < t \leq (m+1)T_u$.

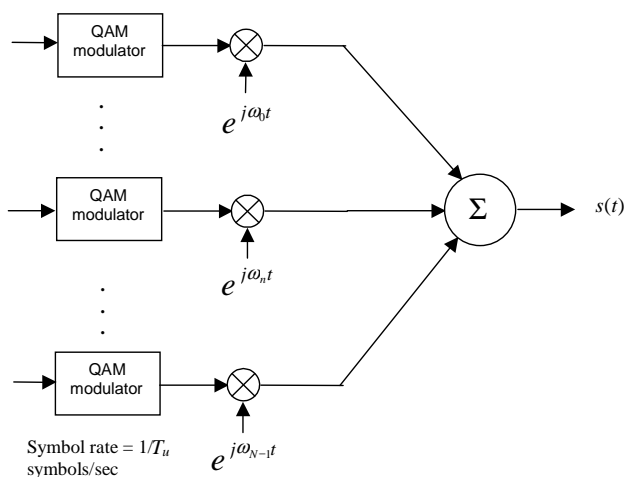


Figure 2: Conceptual representation of OFDM symbol generation

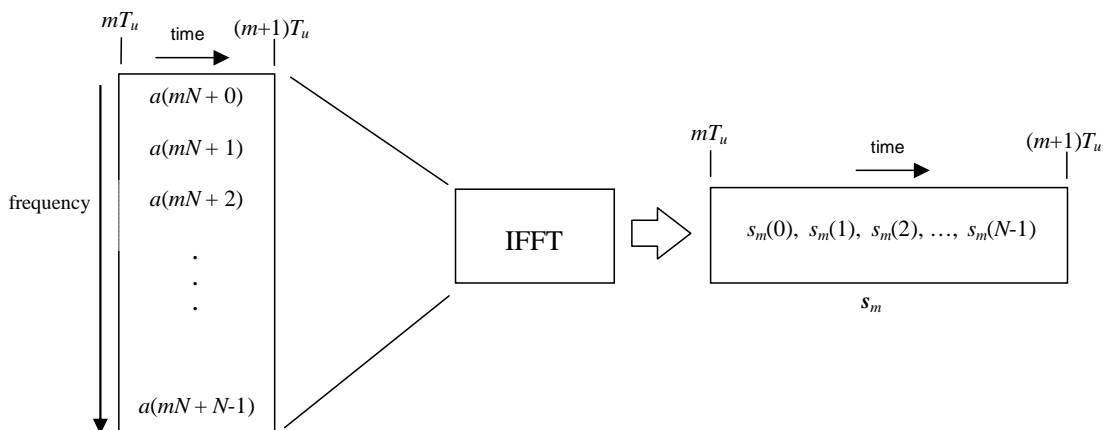


Figure 3: OFDM useful symbol generation using an IFFT

The vector s_m is defined as the useful OFDM symbol. Note that the vector s_m is in fact the time superposition of the N narrowband modulated sub-carriers.

It is therefore easy to realize that, from a parallel stream of N sources of data, each one modulated with QAM useful symbol period T_u , a waveform composed of N orthogonal sub-carriers is obtained, with each narrowband sub-carrier having the shape of a frequency *sinc* function. Figure 4 illustrates the mapping from a serial stream of QAM symbols to N parallel streams, used as frequency domain bins for the IFFT. The N -point time domain blocks obtained from the IFFT are then serialized to create a time domain signal.

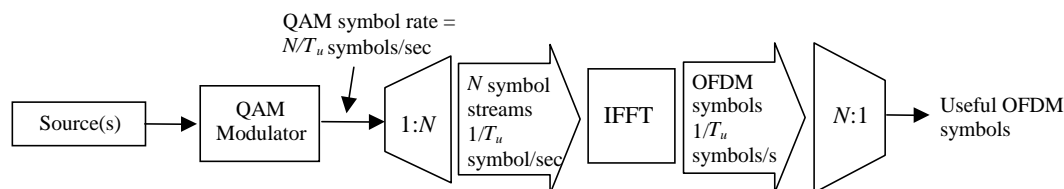


Figure 4: OFDM signal generation chain

4.1.3 Guard Interval

A guard interval may be added prior to each useful OFDM symbol. This guard time is introduced to minimize the inter-OFDM-symbol-interference power caused by time-dispersive channels. The guard interval duration T_g (which corresponds to N_p prefix samples) needs to be sufficient to cover the most of the delay-spread energy of a radio channel impulse response. In addition, such a guard time interval can be used to allow soft-handover.

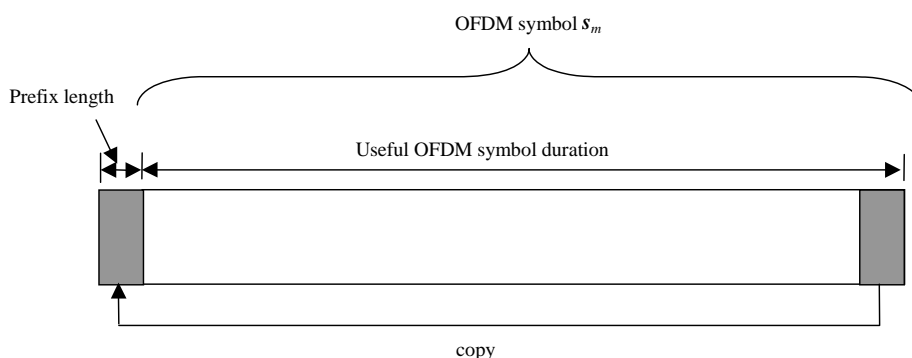


Figure 5: Cyclic prefix insertion

A prefix is generated using the last block of N_p samples from the useful OFDM symbol. The prefix insertion operation is illustrated in figure 5. Note that since the prefix is a cyclic extension to the OFDM symbol, it is often termed cyclic prefix. Similarly, a cyclic postfix could be appended to the OFDM symbol.

After the insertion of the guard interval the OFDM symbol duration becomes $T_s = T_g + T_u$.

The OFDM sampling frequency F_0 can therefore be expressed as:

$$F_0 = \frac{N + N_p}{T_s}$$

hence, the sub-carrier separation becomes:

$$\Delta f = \frac{F_0}{N}$$

It is also worth noting that time-windowing and/or filtering is necessary to reduce the transmitted out-of-band power produced by the ramp-down and ramp-up at the OFDM symbol boundaries in order to meet the spectral mask requirements.

4.1.4 Impact of Guard Interval

The cyclic prefix should absorb most of the signal energy dispersed by the multi-path channel. The entire the inter-OFDM-symbol-interference energy is contained within the prefix if the prefix length is greater than that of the channel total delay spread, i.e.:

$$T_g > \tau$$

where τ is the channel total delay spread. In general, it is sufficient to have most of the energy spread absorbed by the guard interval, given the inherent robustness of large OFDM symbols to time dispersion, as detailed in the next clause.

4.1.5 Impact of Symbol Duration

The mapping of the modulated data symbol onto multiple sub-carriers also allows an increase in the symbol duration. Since the throughput on each sub-carrier is greatly reduced, the symbol duration obtained through an OFDM scheme is much larger than that of a single carrier modulation technique with a similar overall transmission bandwidth. In general, when the channel delay spread exceeds the guard time, the energy contained in the ISI will be much smaller with respect to the useful OFDM symbol energy, as long as the symbol duration is much larger than the channel delay spread, that is:

$$T_s \gg \tau.$$

Although large OFDM symbol duration is desirable to combat time-dispersion caused ISI, however, the large OFDM symbol duration can reduce the ability to combat the fast temporal fading, especially if the symbol period is large compared to the channel coherence time. Thus, if the channel can no longer be considered as constant through the OFDM symbol, the inter-sub-carrier orthogonality loss is introduced and the performance in fast fading conditions are degraded. Hence, the symbol duration should be kept smaller than the minimum channel coherence time. Since the channel coherence time is inversely proportional to the maximum Doppler shift f_d , the symbol duration T_s needs to be, in general, chosen such that:

$$T_s \ll \frac{1}{f_d}.$$

4.1.6 Impact of Inter-Carrier Spacing

Because of the time-frequency duality, some of the time-domain arguments of clause 4.1.5 Impact of Symbol Duration can be translated to the frequency domain in a straightforward manner. The large number of OFDM sub-carriers makes the bandwidth of the individual sub-carriers small relative to the overall signal bandwidth. With an adequate number of sub-carriers, the inter-carrier spacing is much narrower than the channel coherence bandwidth. Since the channel coherence bandwidth is inversely proportional to the channel delay spread τ , the sub-carrier separation is generally designed such that:

$$\Delta f \ll \frac{1}{\tau}.$$

In this case, the fading on each sub-carrier is frequency flat and can be modelled as a constant complex channel gain. The individual reception of the QAM symbols transmitted on each sub-carrier is therefore simplified to the case of a flat-fading channel. Moreover, in order to combat Doppler effects, the inter-carrier spacing should be much larger than the maximum Doppler shift f_d :

$$\Delta f \gg f_d.$$

4.1.7 OFDM Inactive Sub-Carriers

Since the OFDM sampling frequency is larger than the actual signal bandwidth, only a sub-set of sub-carriers is used to carry QAM symbols. The remaining sub-carriers are left inactive prior to the IFFT, as illustrated in figure 6. The split between the active and the inactive sub-carriers is determined based on the spectral constraints, such as the bandwidth allocation and the spectral mask.

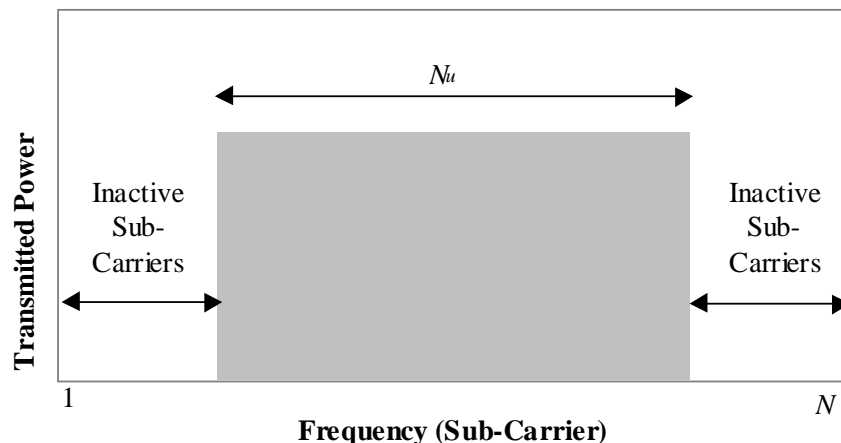
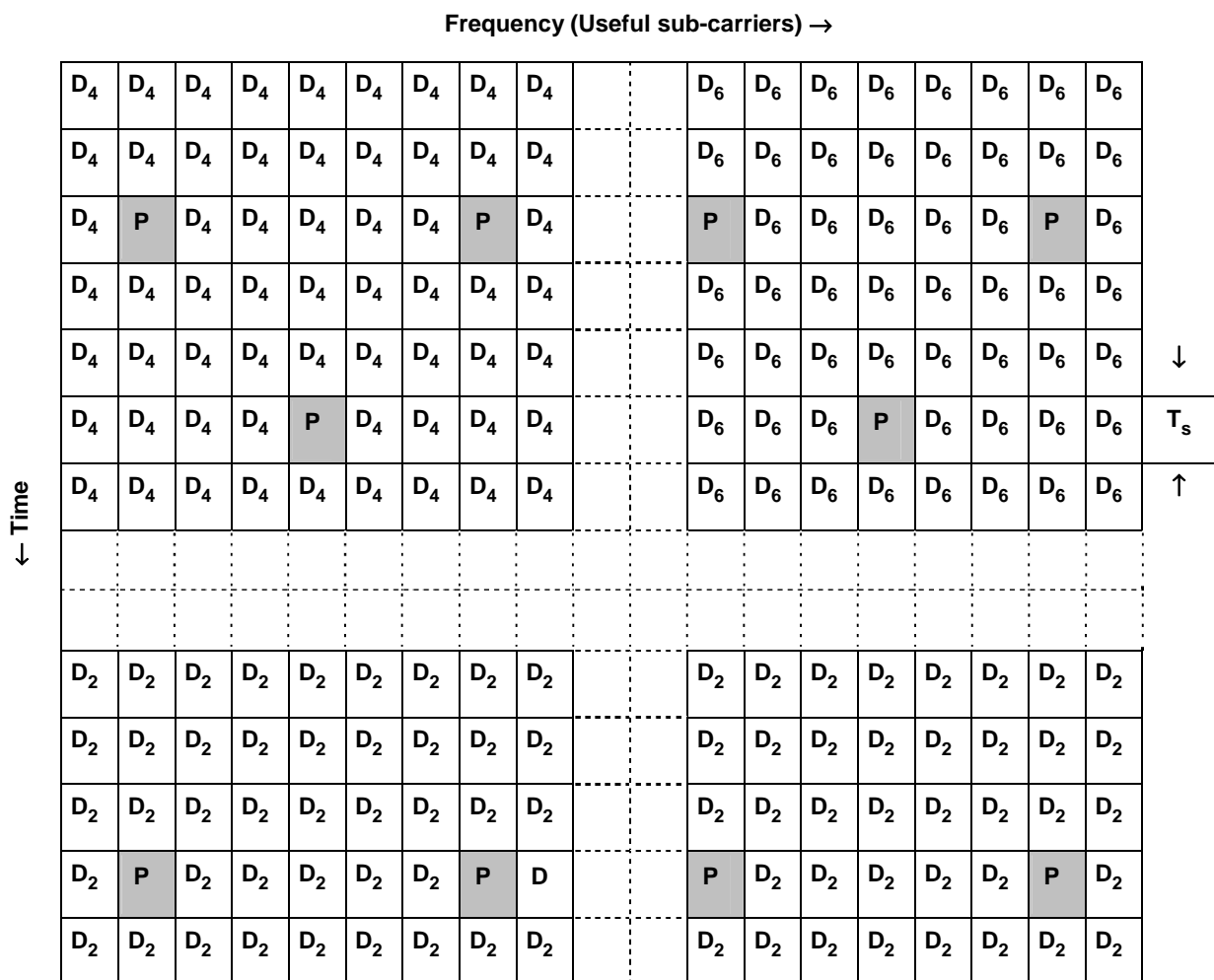


Figure 6: OFDM spectrum with inactive sub-carriers

The N_u modulated sub-carriers (i.e. carrying information), are centered in the N FFT bins, with the remaining inactive sub-carriers, on either side of the modulated sub-carriers.

4.1.8 Time-Frequency Multiplexing

Multiple users can be multiplexed, both in time and in frequency, with pilot and signalling information. In the frequency dimension (i.e. the sub-carrier dimension), users data symbol can be multiplexed on different numbers of useful sub-carriers. In addition, sub-carriers or group of sub-carriers can be reserved to transmit pilot, signalling or other kind of symbols. Multiplexing can also be performed in the time dimension, as long as it occurs at the OFDM symbol rate or at a multiple of the symbol rate (i.e. from one IFFT computation to the other, every $k \cdot T_s$ seconds). The modulation scheme (modulation level) used for each sub-carrier can also be changed at the corresponding rate, keeping the computational simplicity of the FFT-based implementation. This allows 2-dimensional time-frequency multiplexing, of the form shown in figure 7.



P = pilot or signalling, D = data.
 The subscript indicates the modulation level M=2, 4 or 6 (QPSK, 16QAM or 64QAM).

Figure 7: Example of OFDM 2-D structure

4.1.9 OFDM Signal Reception Using the FFT

At the receiver, a computationally efficient Fast Fourier Transform (FFT) is used to demodulate the multi-carrier information and to recover the transmitted data.

4.2 OFDM for Mobile Terrestrial and Satellite Scenario

OFDM has intrinsic features that are generally acknowledged to be well suited to the terrestrial mobile radio environment. In the case of S-DMB, these characteristics are useful in the Complementary Ground Component (CGC) channel. In particular, the following characteristics are worth noting:

- **Time dispersion:** the use of several parallel sub-carriers in OFDM enables longer symbol duration, which makes the signal inherently robust to time dispersion. Furthermore, a guard time may be added to combat further the ISI.
- **Spectral Efficiency:** OFDM is constructed with fully orthogonal carriers, hence allowing tight frequency separation and high spectral efficiency. The resulting spectrum also has good roll-off properties, given that cross-symbol discontinuities can be handled through time windowing alone, filtering alone, or through a combination of the two techniques.

- **Reception:** even in relatively large time dispersion scenarios, the reception of an OFDM signal requires only an FFT implementation in the UE. No intra-cell interference cancellation scheme is required. Furthermore, because of prefix insertion, OFDM is relatively insensitive to timing acquisition errors. On the other hand, OFDM requires to perform frequency offset correction.
- **Extension to MIMO:** since the OFDM sub-carriers are constructed as parallel narrow band channels, the fading process experienced by each sub-carrier is close to frequency flat and therefore, can be modelled as a constant complex gain. This may simplify the implementation of a MIMO scheme if this is applied on a sub-carrier or subset of carrier basis.

5 OFDM and the satellite environment

5.1 Non-Linearity Effects and Predistortion Techniques

When designing wireless communication systems and satellite links in particular, besides the impairments connected with the presence of the radio channel, which can be both frequency and time selective causing strong linear distortion, another severe source of degradation is introduced by High Power Amplifiers (HPA), which can cause non-linear distortion in the transmitted signal, degrading the overall system performance. This occurs when the HPA is driven near saturation, so as to exploit all the available output power and to increase power efficiency. This is particularly true for the OFDM radio interface which is characterized by a rather high Peak-to-Average Power Ratio (PAPR). Besides these factors, the cost of apparatus is another key issue: to properly exploit the expensive equipment, it is necessary to drive it to the limit. This is certainly applicable to the satellite on-board HPA, but it is also true for ground terminals conceived for mass-market, where slight cost reductions per device lead to large overall profits.

A consequence of these facts is that usually the impact of non-linear distortion on the transmitted signal is very strong, as it acts directly on the band-limited pulse stream. The degradation includes amplitude and phase distortion, described by AM/AM and AM/PM characteristics and the generation of in-band and out-band inter-modulation frequencies. These phenomena lead to an increased Adjacent Channel Interference (ACI) due to a widening of the transmitted signal spectrum. In particular, at the receiver each signal constellation point is warped and appears as a cluster, as ISI is generated. These effects can be more or less penalizing for the system depending on the considered HPA characteristics and on the distance from saturation.

The techniques able to counteract non-linear distortion are numerous and include the use of strong channel coding, the use of equalization techniques at the receiver and the use of predistortion techniques at the transmitter. All of these approaches try to mitigate the SNR loss for a given BER, allowing to increase the amplifier output power. Another solution is obviously to back-off from saturation, but as seen before it is not desirable in the majority of cases, where stringent power constraints exist.

The design of a NL compensator should consider a variety of factors, such as coding and modulation schemes, channel estimator subsystem, system service requirements, DC-RF conversion efficiency constraints, system complexity and cost, output power and adjacent channel interference specifications.

5.1.1 Compensation Techniques

In the scientific literature, several techniques have been proposed as means of mitigating non-linear distortion [i.4]:

- The simplest possibility is to back off from saturation, driving the HPA into a more linear region, at the expense of a reduction of the available RF output power, making the link budget fulfilment difficult and of a reduced DC-RF conversion efficiency. Clearly, this solution cannot be applied for on-board amplifiers, given the stringent efficiency and link budget requirements. On the other hand, for on-ground gateway (GW) amplifiers this is an easy way to avoid the unwanted non-linear effects.
- Another solution involves mitigation techniques at the receiver side. This can be efficiently achieved by using equalizers, which try to compensate for the ISI and the constellation point warping. They represent a good choice when there are strict complexity and cost constraints at the transmitter and complexity can be concentrated at the receiver. The main drawback is that the signal is processed after the nonlinear distortion, which hinders the possibility to eliminate the undesirable adjacent channel interference [i.5].

- In order to avoid the generation of adjacent channel interference, the compensation can be introduced before the HPA, so that its output is a linearly amplified version of the original signal. This approach is commonly referred to as *predistortion*, as it consists in processing the signal to be transmitted by means of a nonlinear function, compensating the distortion introduced by the HPA [i.6].

5.1.2 Digital Predistortion Techniques

Predistortion techniques proposed in the literature can be divided into two main classes: *digital* predistorters and *analog* predistorters. Essentially the *waveform (analog) predistorter* compensates for the memory less nonlinearity HPA and it is placed after the pulse shaping filter in RF (or possibly IF) band; the *digital predistorter* is required to compensate a nonlinearity with memory generated by the cascade of the linear pulse shaping filter, which introduces memory and the HPA, which can be conceived as a memory less nonlinearity placed right after the pulse shaping filter at baseband. The digital predistorter exhibits more flexibility in determining the predistorter coefficients than the analog counterpart, since the learning algorithm is programmable in the digital predistorter. This suggests that the digital predistorter can be more dynamically adaptive when system characteristics change as a consequence of a variation in the signal characteristics (i.e. the pdf) or in the power amplifier characteristics (e.g. as a function of temperature, ageing or bias fluctuations).

Digital predistortion techniques can be again subdivided into two categories, namely *data constellation predistortion* and *fractional (or oversampled) predistortion*, according to the location of the compensator. *Data constellation predistorters* are placed in the baseband system before the pulse shaping transmit filter, while *fractional predistorters* are located after the pulse shaping transmit filter. Each of these predistortion techniques can be implemented so as to accomplish a static compensation of HPA nonlinearity effects or to realize an adaptive compensation.

For this study, a fractional predistorter implemented by a gain-based LUT approach is considered [i.7]. The compensator is located after the pulse shaping transmit filter and can correct the average positions of the individual clusters and reduce their variance, bounding the effects of ISI. A square root raised cosine FIR filter is assumed as pulse shaping filter. The output of the pulse shaping filter becomes the input of the predistorter, as in figure 8.

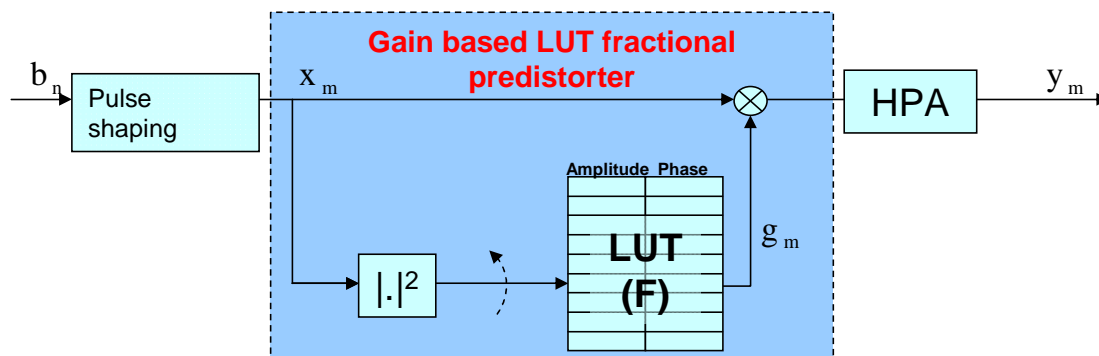


Figure 8: Gain-based LUT fractional predistorter block diagram

Linear in power LUT indexing will be considered, using table entries uniformly spaced along the input signal power range, yielding denser table entries for larger amplitudes. It is characterized by a simple implementation, since it only requires a square module computation and it is particularly effective if the non-linear effects are localized at large amplitudes. The number on LUT entries depends on the allowed complexity at the transmitter, but typical values are from 128 to 1 024. LUT entries computation is based on the inversion of the HPA characteristics that can be properly modelled through analytic expressions.

5.1.3 Multi-Beam Coverage Using OFDM

One of the peculiar characteristics of OFDM, which is largely used in DVB-T, is the relative easiness in deploying Single Frequency Networks (SFNs). This is achieved by synchronizing transmissions from various base stations and by exploiting the guard time to resolve any residual asynchronicity in the signals received from different sources. However, this works if and only if the guard time exceeds the relative delay difference between the two signals. This implies in turn that the cell radius cannot be excessively large, to avoid very large guard times and hence overheads. In other words, terrestrial SFNs based on OFDM have limited cell size and necessitate in general of a large number of base stations.

It is very interesting to note that the application of OFDM in the forward link of a multi-beam antenna coverage from a GEO or non GEO satellite can lead to a much simpler and more effective realization of a SFN. In fact, in a multi-beam antenna coverage, interference from adjacent beams is generated from antenna sidelobes in the direction to the interfered user. In essence, the desired signal and the interference follow exactly the same electro-magnetic path, except for the on-board beamforming and antenna feed circuits. Therefore, the relative delays between desired signal and interference are extremely small, if at all present. In conclusion, the guard time necessary for the realization of an SFN through a multi-beam antenna coverage is much smaller than for the terrestrial case and the beam footprint size is not limited in any way.

6 OFDM feasibility

6.1 Physical Layer Structure in the OFDM Downlink

6.1.1 Physical Channel

Physical channels are defined by a specific carrier frequency, set of orthogonal sub-carriers or sub-bands, time start & stop (or duration), time-frequency interleaving pattern (possibly frequency hopping pattern). Given a carrier frequency, physical channels are therefore mapped onto a specific 2-dimensional area in the time-frequency plane. Before time-frequency interleaving, each physical channel corresponds to a set of sub-bands, while after symbol interleaving, the sub-bands are distributed in a controlled manner across the overall frequency band. The time durations for specific time units for the OFDM HS-DSCH are identical to those of 3GPP and can therefore be measured in integer multiples of WCDMA chips, where the chip rate is 3,84 MHz. The time intervals defined in this configuration are:

- **Radio frame:** Also called an *OFDM frame*, a radio frame is a processing duration which consists of 15 slots. The length of a radio frame corresponds to 38 400 chips (10 msec).
- **Slot:** A slot corresponds to 2 560 chips.
- **HS-DSCH sub-frame:** A sub-frame is the basic time interval for HS-DSCH transmission and HS-DSCH-related signalling at the physical layer. The length of a sub-frame corresponds to 3 slots, i.e. 7 680 chips (2 msec) and is often referred to as a TTI.
- **OFDM symbol:** An OFDM symbol is the signal generated by one inverse FFT in the transmitter, including a cyclic prefix and suffix.

These concepts are illustrated in figure 9. According to the evaluation scenario summarized in table 2, the number of OFDM symbols per TTI is $L=27$ for the Set 1 and $L=12$ for the Set 2. The respective corresponding numbers of OFDM symbols per frame are therefore $K=135$ and $K=60$.

The OFDM signal can be conceptually generated as indicated in figure 10. The *OFDM unit Mapping* refers to the mapping of the individual strings of QAM symbols into *OFDM units*, where such a unit is defined as a group of constellation symbols to be mapped onto a sub-band, a subset of OFDM sub-carriers. The OFDM symbol duration is fixed, with a total of N_u sub-carriers. N_u is equal to the FFT size and therefore includes unused sub-carriers on each extremities of the signal band. The IFFT output vector is multiplexed in the time domain, with a prefix and a suffix, into a vector identified as the OFDM symbol, with (N_u+N_p) samples per symbol, where N_p is equal to the total number of samples in the combination of the prefix and the suffix.

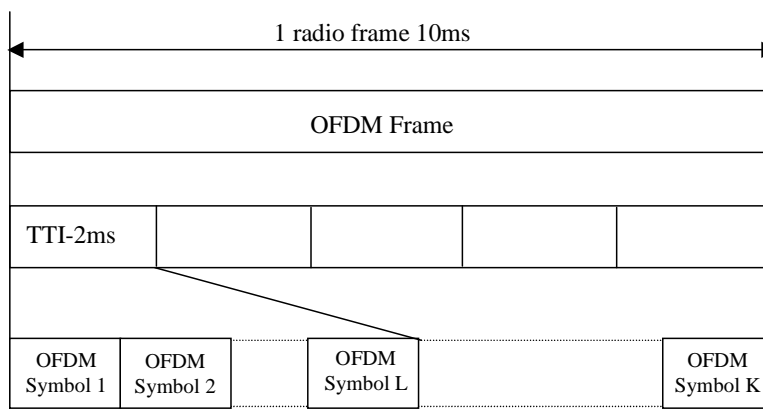


Figure 9: Frame structure for the OFDM HS-DSCH

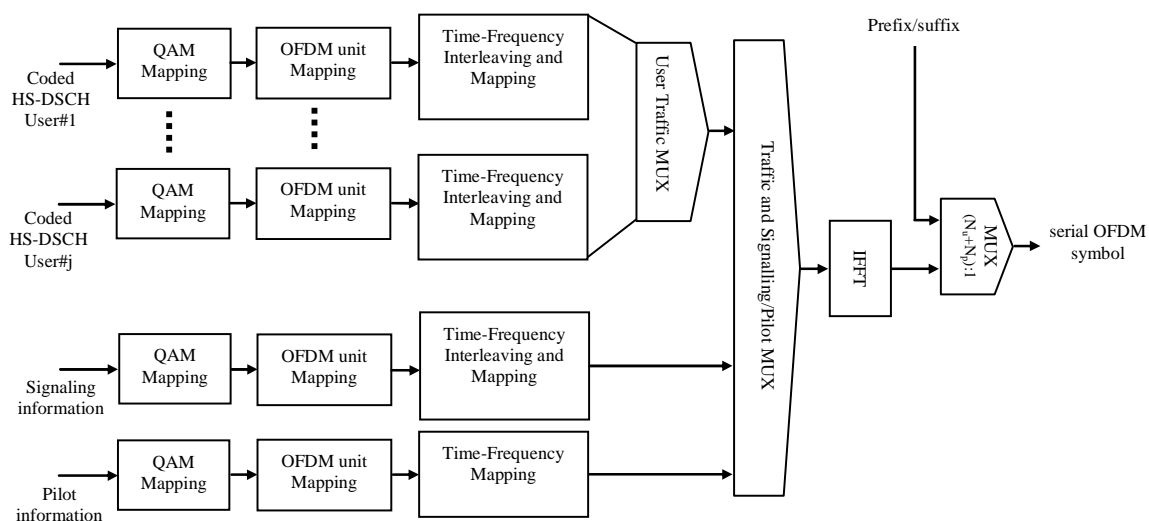


Figure 10: Conceptual representation of the generation of the OFDM signal for multiple HS-DSCHs

6.1.1.1 OFDM Physical Channel Definition

Four types of OFDM physical channels can be defined for HS-DSCH:

- 1) The *OFDM-CPICH* (OFDM common pilot channel): the OFDM unit(s), within a 2 msec sub-frame, containing pilot information. This is a common channel. The pilots are inserted in the time-frequency plane and need to satisfy the 2-D sampling theorem in order to enable reconstruction of the time and frequency varying channel response. The OFDM-CPICH physical channel is not interleaved.
- 2) The *OFDM-TPCCH* (OFDM TPC Channel): the OFDM unit(s), within a slot, containing the uplink TPC bits. This is a shared channel, which is not necessary for pure S-DMB transmission. The specific frequency locations used for signalling could be scattered, in order to benefit from frequency diversity. The time location could be limited to a single OFDM symbol (IFFT/FFT window) per slot, to ease its extraction by the UE. The timing of the dedicated uplink is given by the timing of the dedicated downlink in WCDMA. How to set the uplink timing in case of OFDM downlink is FFS.
- 3) The *OFDM-SCCHs* (OFDM shared control physical channels): the OFDM unit(s), within a 2 msec sub-frame, containing signalling information. This is a shared channel. The specific frequency locations used for signalling should be scattered, in order to benefit from frequency diversity. The time locations can be spread across the sub-frame, while limited to a small number of OFDM symbols (IFFT/FFT windows) to ease extraction of the OFDM-SCCH information by the UE (for instance, the same IFFT/FFT windows already used for the OFDM-TPCCH).

- 4) The *OFDM-PDSCHs* (OFDM physical downlink shared channels): the OFDM unit(s), within a 2 msec sub-frame, not used by the OFDM-CPICH, OFDM-TPCCH or OFDM-SCCH physical channels and dedicated to carry data or higher layer signalling information.

6.1.2 Channel Coding and Multiplexing

In the process of mapping transport blocks onto physical channels, data from multiple users are multiplexed in time and frequency. Figure 11 illustrates the overall transmitter processing chain for the transport blocks of such users. The reference OFDM configuration defines the final part of the transmitter processing chain: the mapping of constellation symbols onto the OFDM physical channels (grey blocks).

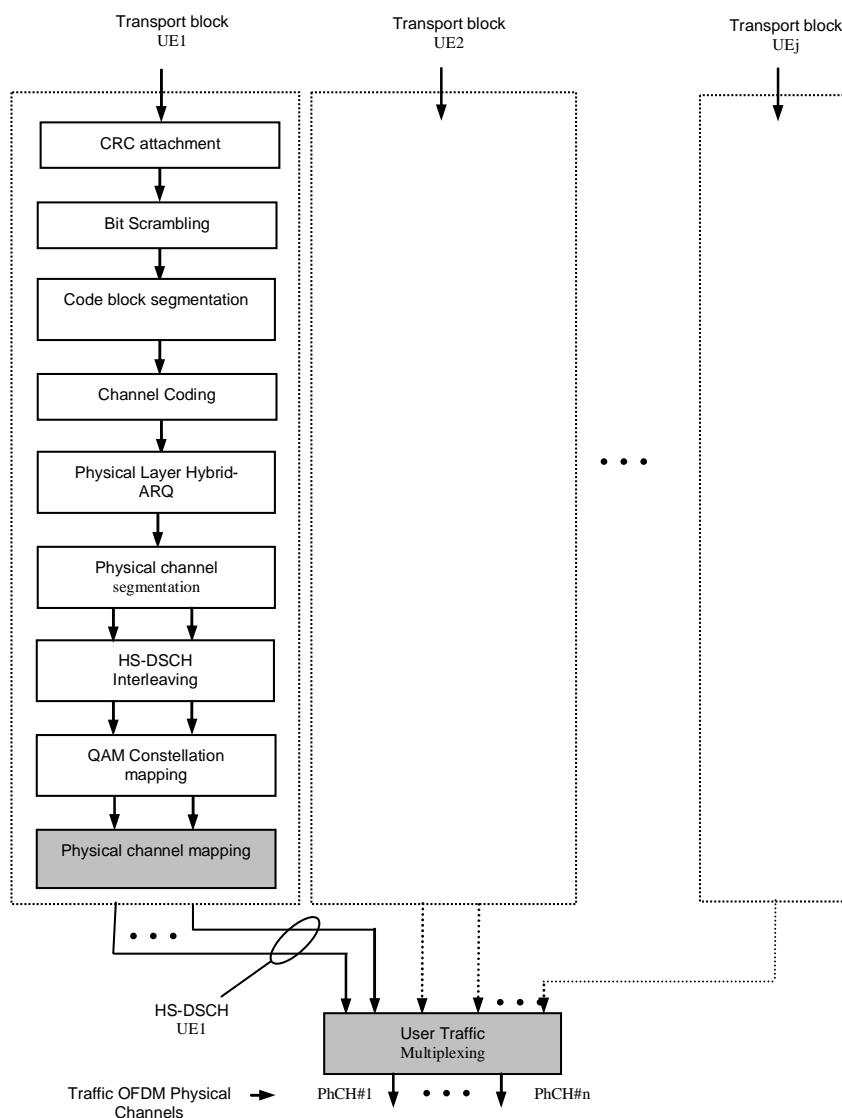


Figure 11: OFDM HS-DSCH transmitter processing chain

Data arrives at the coding unit with a maximum of one transport block every 2 msec TTI. As in HSDPA, there is one transport block of HS-DSCH type per UE. Each traffic transport block is first coded with CRC attachment, then it is bit scrambled, code block segmented, channel coded and processed by HARQ, as indicated in [i.2]. The output of the HARQ block is then segmented into one or more data segments, each one corresponding to a Physical Channel (PhCh). A UE can therefore be assigned multiple physical channels. Each PhCh is interleaved as indicated in [i.2] and each resulting HS-DSCH interleaved data block is mapped to a vector of symbols, taken from the selected QAM constellation. Each QAM symbol vector is then mapped onto a number of OFDM units. Time-frequency interleaving of OFDM units is then applied and results in a mapping of the physical channels on the time-frequency resources. User traffic multiplexing is finally used to multiplex the physical channels from different users, resulting in a number of *Traffic OFDM Physical Channels*.

6.1.3 Physical Channel Mapping

The OFDM frequency band is divided into N_B sub-bands by grouping OFDM sub-carriers. Each sub-band constitutes an *OFDM unit*. This means that in each OFDM symbol interval at most N_B parallel OFDM units can be transmitted.

Three different essential steps for the physical channel mapping are identified:

- 1) The QAM symbols, obtained in the constellation mapping, are mapped onto a number of OFDM units. Each PhCh is inserted by row into the time-frequency matrix (figure 12). N_B physical channels are multiplexed in a TTI.
- 2) The OFDM unit interleaver permutes the QAM symbols in the consecutive OFDM units. In other words, an inter-columns permutation is performed.
- 3) The time-frequency (T-F) mapping of OFDM units puts each OFDM unit at a unique position in available time-frequency space. Each physical channel should have a separate, non-overlapping time-frequency mapping. The OFDM unit interleaver and time-frequency mapping constitute together a time-frequency interleaver of OFDM units.

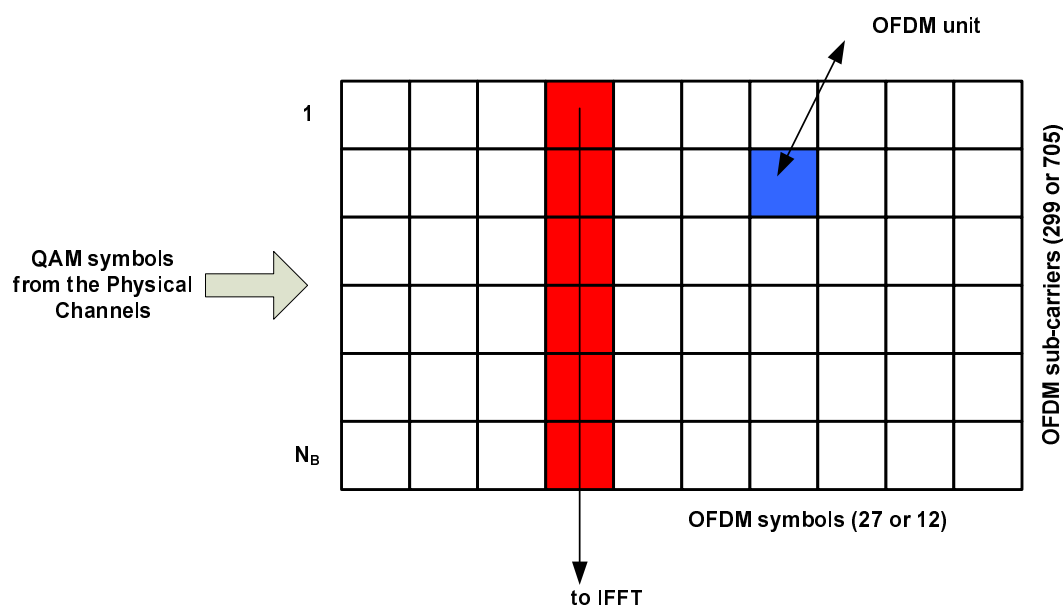


Figure 12: OFDM time-frequency channel mapping

After the three steps, each column is ready to feed the IFFT block to constitute an useful OFDM symbol.

6.1.4 User Traffic Multiplexing Solutions

The user traffic multiplexing is performed by allocating to each physical channel a separate pattern for the T-F mapping of OFDM units. All T-F mapping patterns in a cell should be orthogonal, to avoid the cross-interference between the physical channels. Choosing the T-F pattern is a tool to combat frequency selective fading and to minimize the inter-cell interference. This T-F mapping pattern can be used to support frequency scheduling.

Some possible efficient solutions, satisfying to a large extent the above requirements for both parameter sets, are described in the following clause.

6.1.4.1 Solution based on a generic Costas sequence

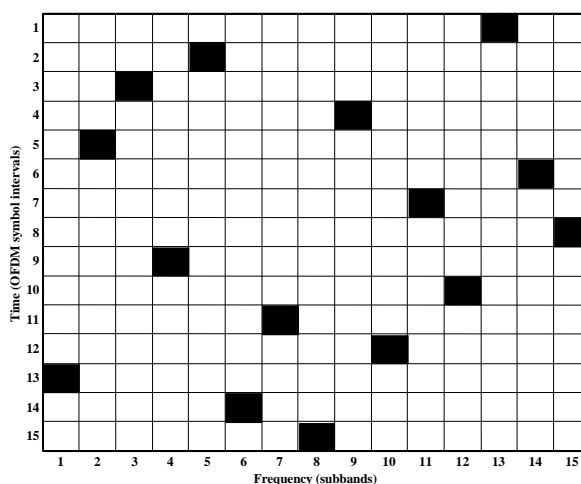
The solution for user traffic multiplexing described in this clause achieves concurrently three goals: a) maximize the minimum (Lee) distance between any two points on the time-frequency grid; b) minimize the maximum normalized periodic Hamming cross-correlation between any two T-F patterns and c) minimize the maximum side-lobe of normalized periodic Hamming auto-correlation of each T-F pattern.

The available Costas sequences for the T-F mapping are listed in table 1. The Costas sequences are derived from [i.8].

Table 1: Costas sequences for T-F mapping

Number of OFDM units, N_B	Costas sequence description
5	Obtained from T_4 in the Galois field GF(19) with primitive $\alpha=14$
10	Obtained from L_3 in the Galois field GF(13) with primitive $\alpha=7$
15	Obtained from L_2 in the Galois field GF(7) with primitive $\alpha=3$

In the following, an example of Costas sequence is reported for 15 OFDM units assuming the parameter set cases listed in table 2. A generic T-F pattern (TFP_{generic}) is shown in figure 13, as a sequence of indices of the sub-bands used for the transmission within a TTI.

**Figure 13: A generic time-frequency pattern (from T_4 Costas sequence of length 15)**

For the Set 2 configuration, the first pattern is obtained by discarding the last three symbols of the generic Costas sequence, in order to obtain the patterns of length $N_{OFDM}=12$. For the parameter Set 1, the first pattern is obtained by extending the generic Costas sequence by the reversed first 12 symbols of the same generic pattern, in order to obtain the patterns of length $N_{OFDM}=27$. Mathematically, it can be described as:

$$TFP_0^{(\text{ParSet2})} = TFP_{\text{generic}}(1:12),$$

$$TFP_0^{(\text{ParSet1})} = [TFP_{\text{generic}} \ TFP_{\text{generic}}(12:-1:1)].$$

For the parameter Set 2, the first two T-F patterns are given by:

$$TFP_0^{(\text{ParSet2})} = [13 \ 5 \ 3 \ 9 \ 2 \ 14 \ 11 \ 15 \ 4 \ 12 \ 7 \ 10],$$

$$TFP_1^{(\text{ParSet2})} = [14 \ 6 \ 4 \ 10 \ 3 \ 15 \ 12 \ 1 \ 5 \ 13 \ 8 \ 11].$$

For the parameter Set 1, the first two T-F patterns are given by:

$$TFP_0^{(\text{ParSet1})} = [13 \ 5 \ 3 \ 9 \ 2 \ 14 \ 11 \ 15 \ 4 \ 12 \ 7 \ 10 \ 1 \ 6 \ 8 \ 10 \ 7 \ 12 \ 4 \ 15 \ 11 \ 14 \ 2 \ 9 \ 3 \ 5 \ 13],$$

$$TFP_1^{(\text{ParSet1})} = [14 \ 6 \ 4 \ 10 \ 3 \ 15 \ 12 \ 1 \ 5 \ 13 \ 8 \ 11 \ 2 \ 7 \ 9 \ 11 \ 8 \ 13 \ 5 \ 1 \ 12 \ 15 \ 3 \ 10 \ 4 \ 6 \ 14].$$

In general, all patterns in the set are obtained from the *first* pattern in the set by *all the different cyclic shifts in the frequency domain*.

6.2 Spectrum Compatibility

To minimize the impact of the introduction of OFDM in S-DMB systems and to ensure the coexistence of OFDM with WCDMA standard, the OFDM carriers should be spectrally compatible with current WCDMA UMTS carriers.

The OFDM signal spectrum should be shaped prior to transmission to meet the UMTS spectrum emission mask. The OFDM spectrum roll-off can be controlled at baseband by using the windowing and overlapping of consecutive OFDM symbols, as illustrated in figure 14.

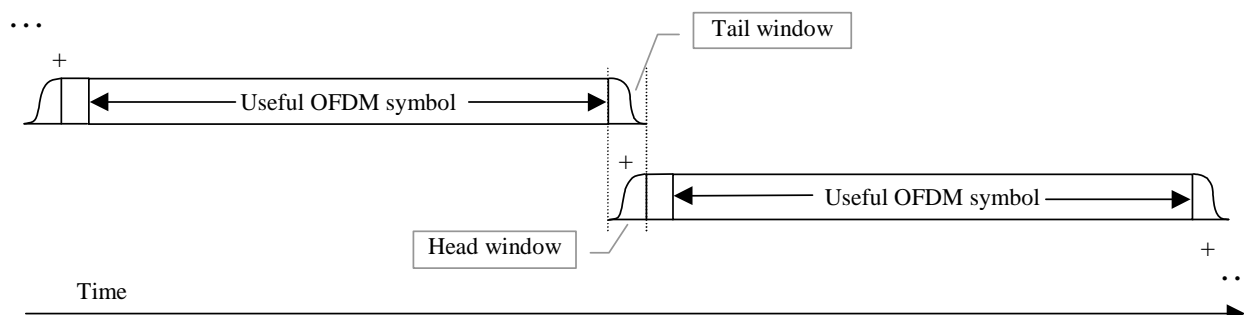


Figure 14: Windowing in consecutive OFDM symbols

Several different windowing functions can be used. The spectrum obtained using a straightforward trapezoidal window (i.e. using linear head and tail weighting functions) is illustrated in figures 15 and 16, for the two sets of OFDM parameters proposed in table 2. In both figures, the spectrum of an OFDM signal without windowing is also illustrated. It is clear that in the absence of a spectrum shaping method, the intrinsic spectrum of the OFDM signal would not meet the required emission mask. According to figures 15 and 16, using a window size in the range of 20 samples to 30 samples for the overlapping head and tail windows should be sufficient to meet the UMTS spectrum emission mask.

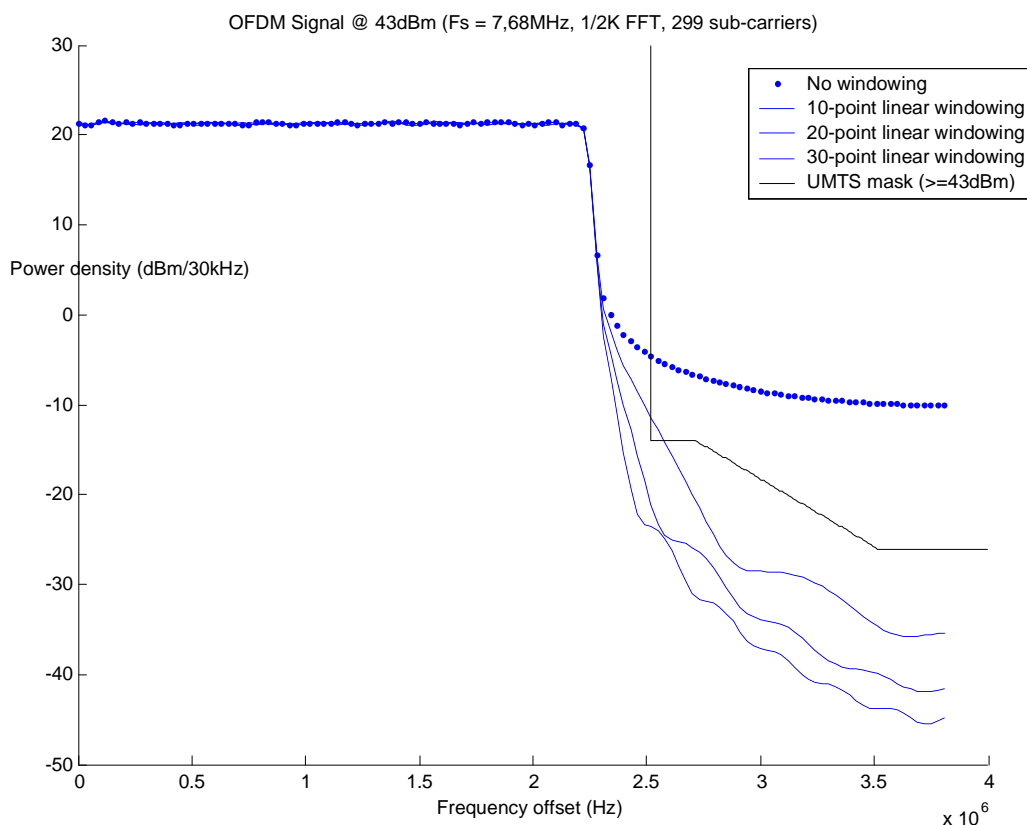


Figure 15: OFDM spectrum for parameter Set 1 (@ 43dBm)

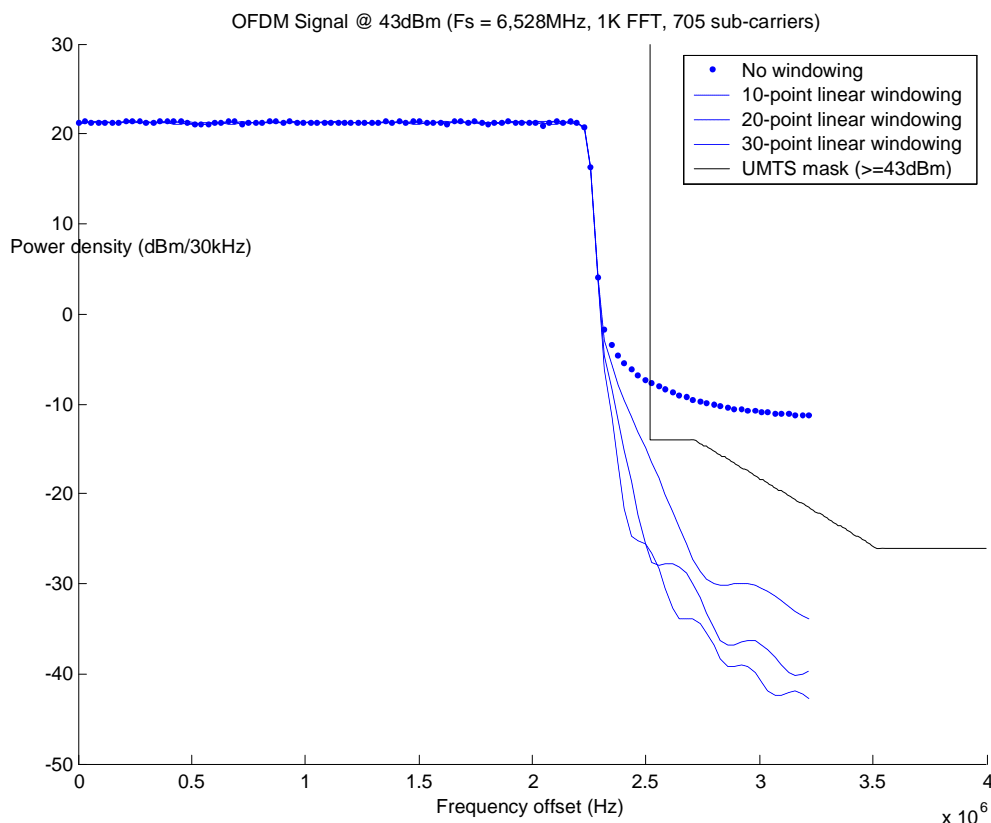


Figure 16: OFDM spectrum for parameter Set 2 (@ 43dBm)

7 OFDM Evaluation Scenario

7.1 Reference System Scenario for OFDM S-DMB Analysis

This clause describes reference scenarios for analysing the OFDM radio interface in the context of high speed data services for S-DMB. An initial reference system configuration is proposed to evaluate an OFDM downlink, as an alternative to a WCDMA downlink. In the proposed configuration, a bundle of high speed data services are provided through the use of a separate 5 MHz downlink carrier, supporting the OFDM HS-DSCH transmission. The reference architecture is shown in figure 17, where the uplink connection is assumed to be going through the terrestrial air interface.

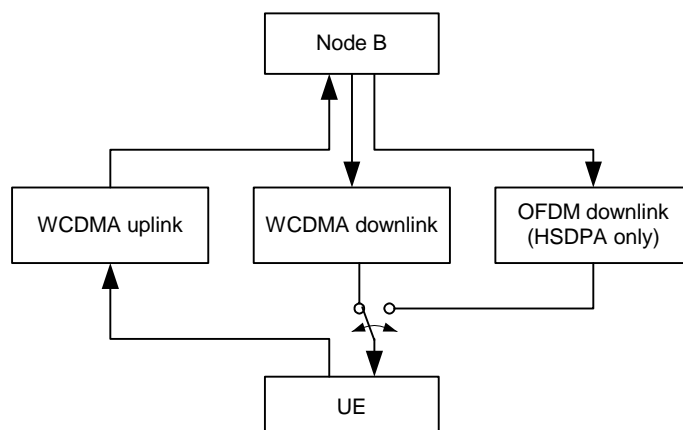


Figure 17: Reference link diagram for OFDM HS-DSCH transmission

The separate OFDM DL carrier is operated using HSDPA features, such as link adaptation and HARQ. It is assumed that network access is performed through the WCDMA architecture and handover to the OFDM carrier occurs, when needed, for background and streaming S-DMB data services. Therefore, a UE with OFDM HS-DSCH receiving capabilities also need to have WCDMA receiving capabilities. Based on this initial reference scenario, a UE with OFDM HS-DSCH receiving capabilities is not required to receive the WCDMA and OFDM carriers simultaneously.

Since the objective of the study item is to evaluate the potential benefits of OFDM as a radio interface for S-DMB systems, the evaluation should be decoupled from the impact of other factors. To achieve this, the proposed OFDM HSDPA-only carrier is compared to an equivalent HSDPA-only carrier. This is shown in figure 18.

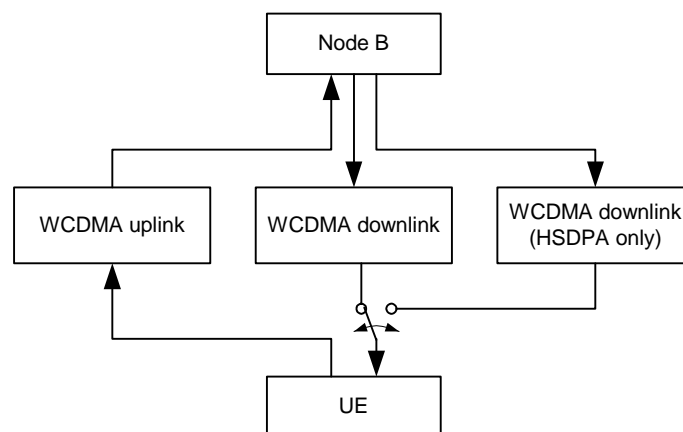


Figure 18: Reference link diagram for HSDPA-only transmission

7.2 Reference OFDM configurations for the evaluation

According to [i.1], two sets of reference OFDM configuration parameters are listed in table 2. The main difference with respect to the terrestrial counterpart of this study will consist in the introduction of the space segment, including linear and non linear distortion sources. This may have a very significant impact on performance unless smart modulation, predistortion and equalization techniques are adopted.

Table 2: Reference OFDM configuration parameter sets

Parameters	Set 1	Set 2
TTI duration (msec)	2	2
FFT size (points)	512	1 024
OFDM sampling rate (Msamples/sec)	7,68	6,528
Ratio of OFDM sampling rate to UMTS chip rate	2	17/10
Guard time interval (cyclic prefix) (samples/ μ sec)	56 / 7,29 57 / 7,42 (see note 1)	64/9,803
Sub-carrier separation (kHz)	15	6,375
# of OFDM symbols per TTI	27	12
OFDM symbol duration (μ sec)	73,96/74,09 (see note 2)	166,67
# of useful sub-carriers per OFDM symbol	299	705
OFDM bandwidth (MHz)	4,485	4,495
NOTE 1: Requires one extra prefix sample for 8 out of 9 OFDM symbols.		
NOTE 2: Depending on guard interval duration.		

The parameter set 1 consists of 9 OFDM symbols that fit into a 0,667 μ s timeslot. The useful symbol duration is equal to 512 samples. The guard interval is equal to 56 samples for the 0th symbol and 57 samples for symbols 1..8 of every timeslot, as illustrated in figure 19. The actual position of the 56-sample GI symbol is believed to be inconsequential as long as it is known by both the transmitter and receiver. It should be noted that spectral shaping of the OFDM signal is required for out-of-band emission compliance.

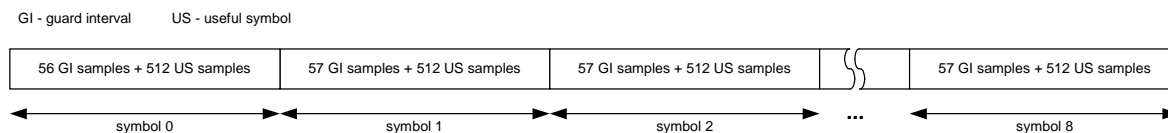


Figure 19: Temporal structure of the OFDM signal (one timeslot), parameter set 1

8 Simulation Results

8.1 Uncoded System Performance

8.1.1 AWGN Channel

First of all, the OFDM interface is considered in the AWGN channel for both sets (refer to table 2). The simulation results are reported in figure 20 adopting both the QPSK and 16QAM modulation scheme.

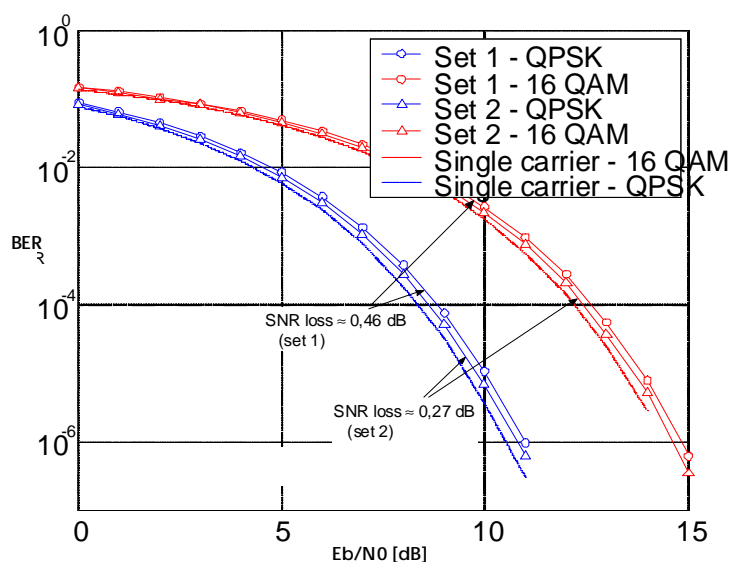


Figure 20: Uncoded OFDM performance in AWGN channel

Independently from the modulation format, the OFDM scheme has a slightly BER degradation with respect to the single carrier case. This degradation is perfectly expectable taking into account the fact that the cyclic prefix is discarded at the receiver side. In other words, from the receiver point of view, the cyclic prefix represents only an energy loss and it is quantifiable as follows:

$$SNR_{loss} = \frac{N + N_p}{N}$$

Substituting the parameter set values, it can be noted the Set 2 SNR_{loss} is minor than the Set 1 case. In particular, the Set 2 SNR_{loss} is about 0,27 dB, whereas the Set 1 value is in the order of 0,46 dB.

8.1.2 Non-linear channel

The introduction of the satellite TWTA is considered. Figure 21 reports the Set 1 BER performance for several IBO values without predistortion techniques for QPSK and 16QAM modulation scheme. For IBO=20 dB (see note), both the modulation formats confirm the BER degradation discussed in the previous clause. Concerning the QPSK scheme, for IBO=15 dB, the performance loss at BER=10⁻⁴ is in the order of 0,5 dB, whereas for IBO=2 dB or 3 dB, a floor is notable at BER=10⁻³. On the other hand, the 16QAM modulation format is more sensitive to non-linearity effects. In particular, for IBO=15 dB, the performance loss at BER=10⁻⁴ is already in the order of 2 dB, while for IBO=2 dB or 3 dB, the BER is fixed to 0,06 ÷ 0,07.

NOTE: The HPA non-linearity is negligible.

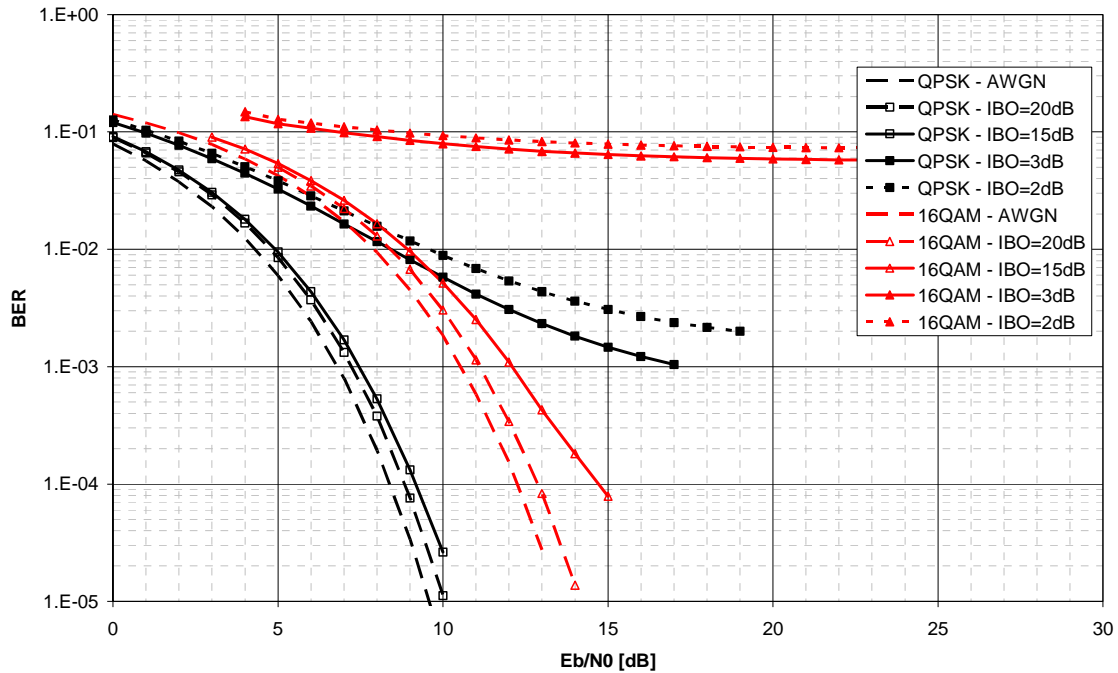


Figure 21: Set-1 uncoded OFDM performance for several IBO values without predistortion techniques

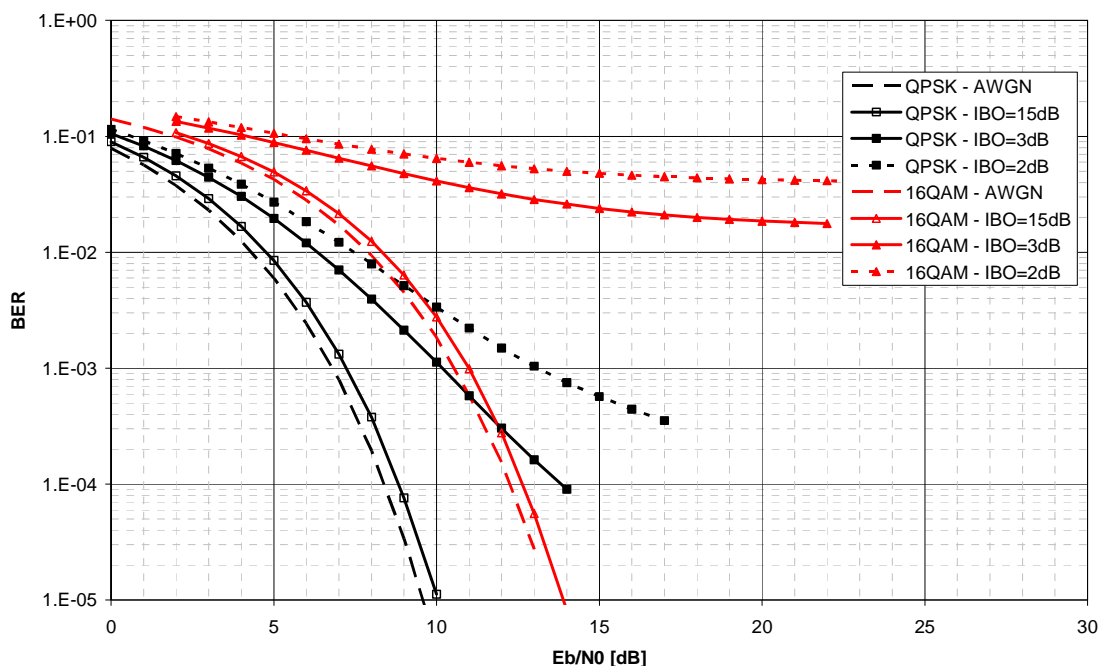


Figure 22: Set-1 uncoded OFDM performance for several IBO values with fractional predistortion

The fractional predistortion technique is introduced in figure 22. For both modulations and IBO=15 dB, it can be noted that the developed predistorter completely compensates the HPA non-linear effects. As far as the QPSK scheme is concerned, the removal of the BER floor is quite evident for IBO=3 dB and improved performance is notable for IBO=2 dB. On the other hand, the 16QAM performance gain with the fractional predistorter is less appreciable than the QPSK scheme. Nevertheless, looking at the E_b/N_0 range where a coded system works (around 4 dB to 6 dB), the same BER (i.e. 10^{-1}) is achieved with an improvement of 2 dB to 3 dB.

8.2 WCDMA Coding Performance

The information payload and coding rate are compliant with the grey line shown in table 3 that is extracted from [i.1] as reference scenarios for HSDPA and OFDM comparison purpose. More precisely, the downlink capacity is assumed to be entirely available for HS-DSCH transfers, i.e. either 15 OFDM units or 15 HSDPA codes are available for data services.

Table 3: Information bit payload and code block sizes for each transport format assuming 15 WCDMA or OFDM units allocated to a single user per 2 ms TTI

Modulation	Code Rate	Information Bit Payload	24-bit CRC Addition	Code Block Segmentation	R=1/3 Turbo Encoding	Rate Matching
QPSK	1/3	4 800	4 824	1x4 824	14 484	14 400
QPSK	1/2	7 200	7 224	2x3 612	21 696	14 400
QPSK	2/3	9 600	9 624	2x4 812	28 896	14 400
QPSK	3/4	10 800	10 824	3x3 608	32 508	14 400
QPSK	4/5	11 520	11 544	3x3 848	34 668	14 400
16QAM	1/3	9 600	9 624	2x4 812	28 896	28 800
16QAM	1/2	14 400	14 424	3x4 808	43 308	28 800
16QAM	2/3	19 200	19 224	4x4 806	57 720	28 800
16QAM	3/4	21 601	21 625	5x4 325	64 935	28 800
16QAM	4/5	23 041	23 065	5x4 613	69 255	28 800

As specified in [i.3], in this example the coded sequence, i.e. 14 400 coded bits, is mapped onto QPSK symbols and segmented in blocks of 480 QAM symbols to form the 15 OFDM units or the 15 HSDPA PhChs feeding the channel mapping and multiplexing blocks.

The OFDM T-F mapping and multiplexing functionality is depicted in figure 23 for the parameter Set 1. The dual operation for the HSDPA interface is reported in figure 24.

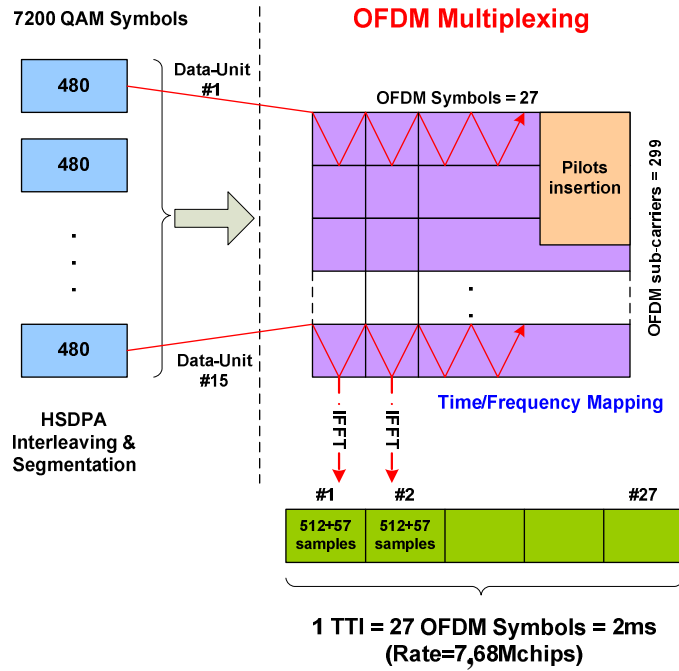


Figure 23: OFDM multiplexing structure (Set 1)

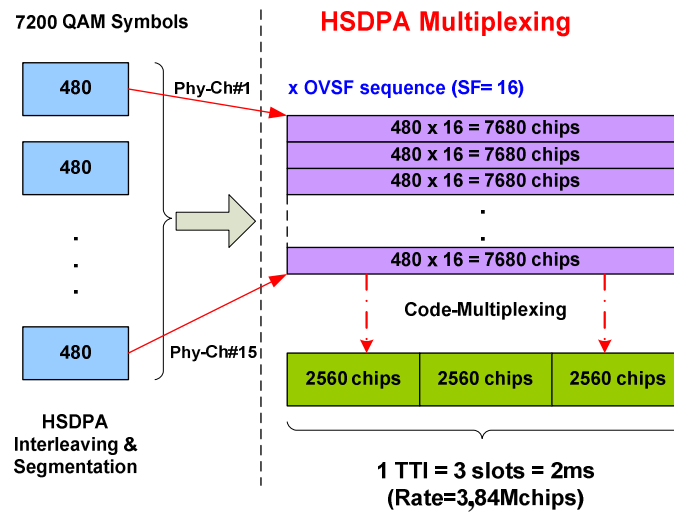


Figure 24: HSDPA multiplexing structure

8.2.1 Non selective Rice fading

Simulation results are reported for both OFDM and HSDPA radio interface in presence of non linear distortion and non selective Rice fading.

The first comparison between OFDM and HSDPA is reported in figure 25. Assuming ideal interleaving, OFDM and HSDPA are compared with different IBO values (see note) and Rice factors, $K=10$ dB or $K=5$ dB. From these curves, several interesting observations can be drawn. Firstly, considering the AWGN performance, the OFDM loss with respect to the HSDPA curve is of approximately 0,4 dB. These losses are due to the guard interval insertion, as discussed in clause 8.1.1 AWGN Channel. Considering the ideal interleaving case for different Rice factors, the loss of the OFDM case rises to 0,9 dB. This has to be related to the way ideal interleaving is obtained. Indeed, with the considered parameters the same channel coefficient is applied to one QPSK-modulated symbol for the HSDPA case and to 299 consecutive sub-carriers for the OFDM case, inducing longer fade events. Finally, looking at the IBO=2 dB case, the non-linearity impact is the same on OFDM and HSDPA. In fact, comparing the distance between the curves with IBO=15 dB and IBO=2 dB, the performance degradation is about 0,8 dB for both cases.

NOTE: IBO=15 dB corresponds HPA working in linear region, whereas IBO=2 dB means very close to the saturation region.

The terminal mobility effects on PER performance are shown in figure 26. Results for three speeds, namely 100 km/h, 200 km/h and 2 000 km/h are reported. Interestingly, the distance between the two sets is again 0,4 dB as for the AWGN case. In fact, now the channel diversity (or the correlation between consecutive channel coefficients) is the same for both systems, so the distance between PER performance is only caused by the guard time energy loss.

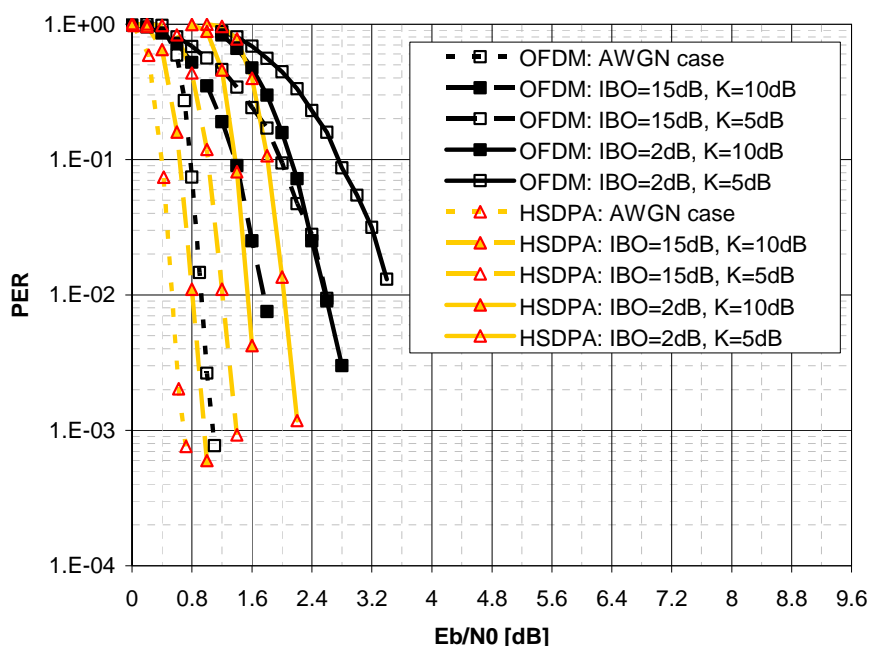


Figure 25: OFDM vs. HSDPA for 1/3-QPSK with ideal interleaving
Different IBO values and Rice factor are reported

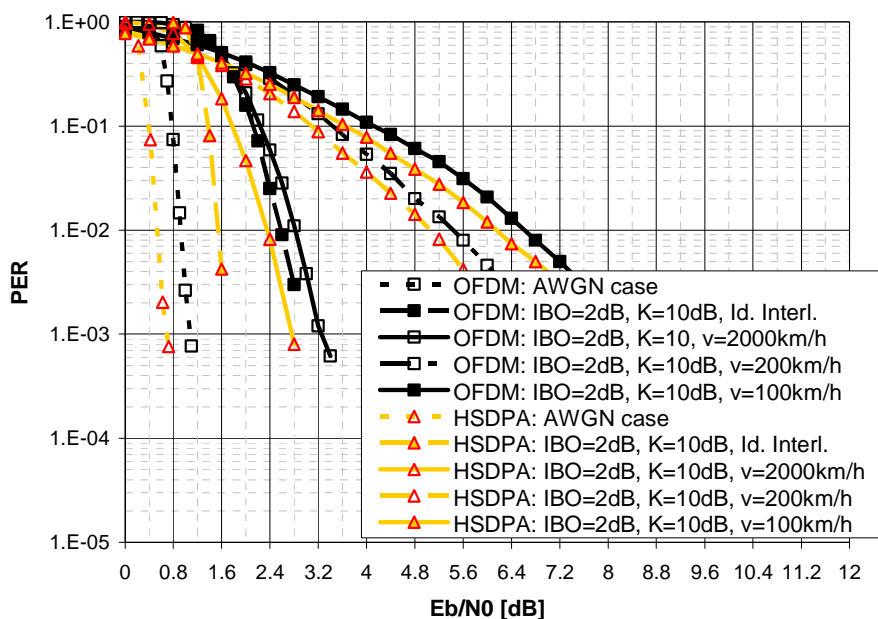


Figure 26: OFDM vs. HSDPA for 1/3-QPSK for several terminal speed IBO=2 dB and Rice factor K=10 dB

8.2.2 Frequency Selective Channel

After the comparison in a time selective frequency flat channel, in the following the OFDM and HSDPA radio interfaces are simulated in a multi-path environment [i.9]. The considered frequency selective channels are compliant with the specifications carried out in the IST-MAESTRO Project. For the sake of completeness, the selected S-DMB propagation channels are reported below.

Table 4: S-DMB propagation channel, Case-1

Case-1: Satellite LOS with many rays		
Delay [ns]	Power [dBm]	Rice Factor [dB]
0	-91,9	10
195,3	-106,3	-inf
260,4	-110,1	-inf
846,3	-112,5	-inf
1 171,9	-110,2	-inf
1 953,1	-112,5	-inf
2 734,3	-112,5	-inf

Table 5: S-DMB propagation channel, Case-2

Case-2: Satellite LOS with few rays		
Delay [ns]	Power [dBm]	Rice Factor [dB]
0	-91,8	7
130,2	-110,1	-inf

Table 6: S-DMB propagation channel, Case-3

Case-3: Satellite NLOS with many rays		
Delay [ns]	Power [dBm]	Rice Factor [dB]
0	-108,5	-inf
195,3	-110,9	-inf
260,4	-106,6	-inf
390,6	-109,3	-inf

Table 7: S-DMB propagation channel, Case-4

Case-4: Satellite+3 CGCs (without processing delay) – street canyon		
Delay [ns]	Power [dBm]	Rice Factor [dB]
0	-90,9	7
1 367,2	-62,3	-inf
1 627,6	-65,7	-inf
1 692,7	-66,9	-inf
1 822,9	-67,0	-inf
2 148,4	-80,6	-inf
2 213,5	-80,4	-inf
3 515,6	-81,1	-inf
5 078,0	-66,5	-inf
6 835,8	-81,5	-inf

Table 8: S-DMB propagation channel, Case-5

Case-5: Satellite+3 CGCs (without processing delay) – open area		
Delay [ns]	Power [dBm]	Rice Factor [dB]
0	-91,8	7
1 692,7	-67,8	-inf
1 757,8	-80,7	-inf
2 278,6	-67,5	-inf
2 343,7	-72,8	-inf
2 408,8	-69,6	-inf
3 190,0	-73,1	-inf
8 203,0	-74,8	-inf
8 268,1	-78,4	-inf
8 788,9	-81,6	-inf

Table 9: S-DMB propagation channel, Case-6

Case-6: Satellite+3 IMRs (without processing delay) – large delay		
Delay [ns]	Power [dBm]	Rice Factor [dB]
0	-91,7	7
8 203,0	-74,4	-inf
9 179,5	-86,3	-inf
10 872,2	-85,4	-inf
11 002,4	-86,8	-inf
12 630,0	-86,4	-inf
18 098,6	-89,2	-inf
18 424,1	-73,6	-inf
18 498,2	-88,6	-inf
22 981,3	-89,3	-inf

Table 10: S-DMB propagation channel, Case-7

Case-7: Satellite NLOS only		
Delay [ns]	Power [dBm]	Rice Factor [dB]
0	-109,5	-inf
130,2	-122,0	-inf
195,3	-124,1	-inf
325,5	-126,6	-inf
390,6	-130,8	-inf
1 106,8	-128,6	-inf

Ideally assuming a terminal speed of 1 000 km/h, the comparison between OFDM and HSDPA is reported in figures 27 and 28 for all S-DMB frequency selective channels under investigation.

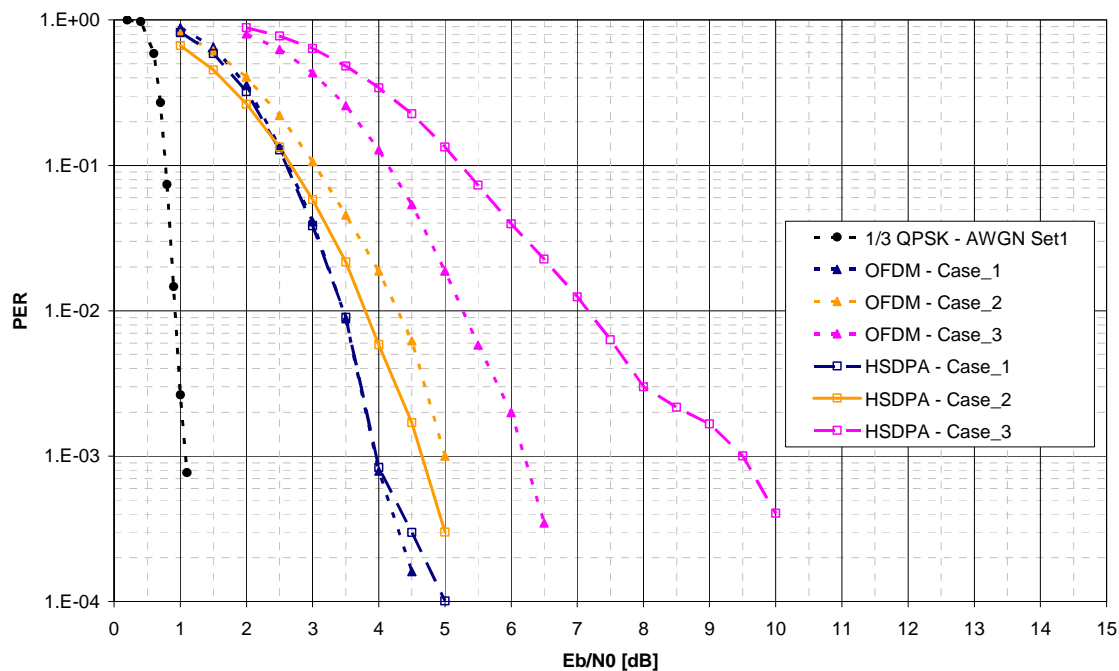


Figure 27: OFDM vs. HSDPA comparison for S-DMB multi-path channels: Case-1, Case-2 and Case-3. Terminal speed set to 1 000 km/h

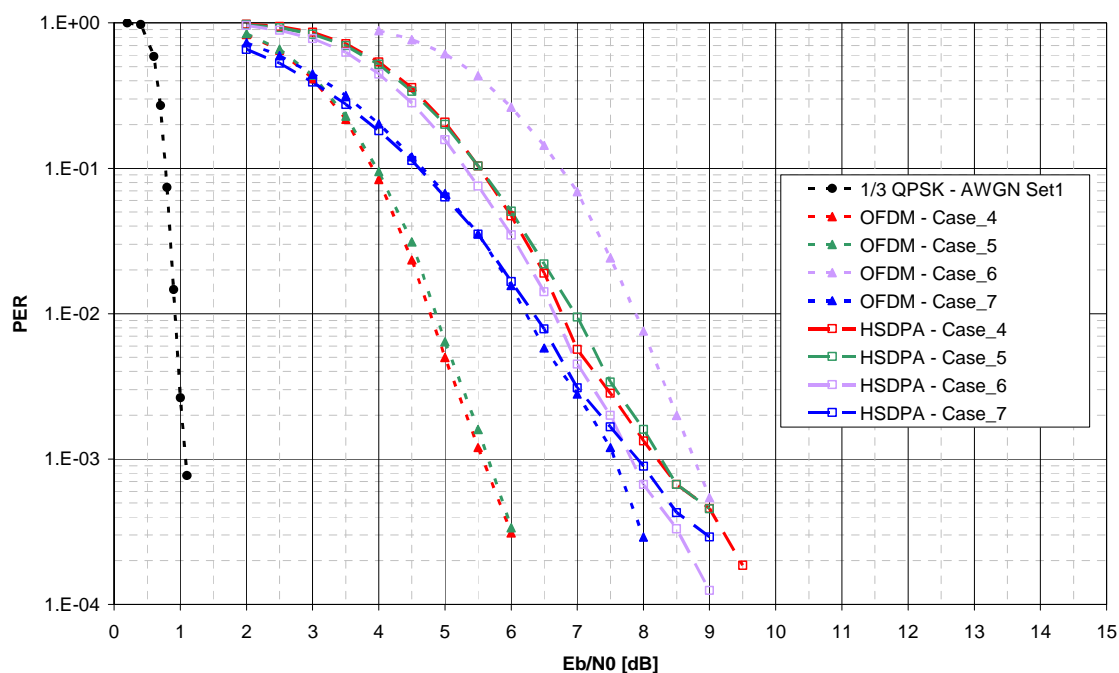


Figure 28: OFDM vs. HSDPA comparison for S-DMB multi-path channels: Case-4, Case-5, Case-6 and Case-7. Terminal speed set to 1 000 km/h

The three cases shown in figure 27 do not consider the presence of the CGCs. In particular, for the Case-1 and Case-2, the reflected rays are almost two orders of magnitude weaker than the satellite link and thus it can be noted that the PER performance are very similar to the non-selective Rice fading channel case. Different considerations need to be pointed out for the Case-3 (Satellite NLOS with many rays). In this configuration, the OFDM gain with respect to the HSDPA radio interface is more significant. In other words, in this case the frequency diversity is fully exploited by OFDM, which leads to a performance gain in the order of 3 dB at $PER=10^{-3}$.

The results considering the remaining multi-path channels are reported in figure 28 (satellite and IMR paths) and confirm the OFDM performance gain with respect to the HSDPA solution. Interesting observations can be drawn for the Case-5 and Case-6 results. In fact, looking at the maximum delay spread in tables 8 and 9, it can be noted that it is always greater than the foreseen guard interval of the Set-1 configuration reported in table 2. Nevertheless, the OFDM performance is still good and the degradation is about 2 dB for the Case-5, in which the maximum delay spread is almost three times the cyclic-prefix length.

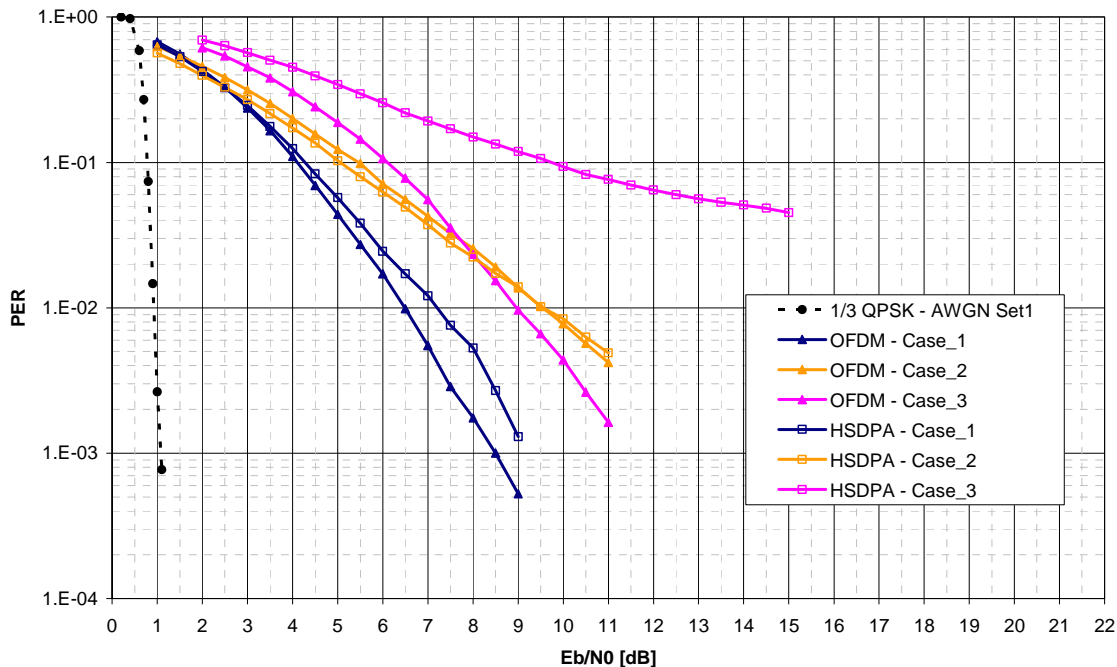


Figure 29: OFDM vs. HSDPA comparison for S-DMB multi-path channels: Case-1, Case-2 and Case-3. Terminal speed set to 100 km/h

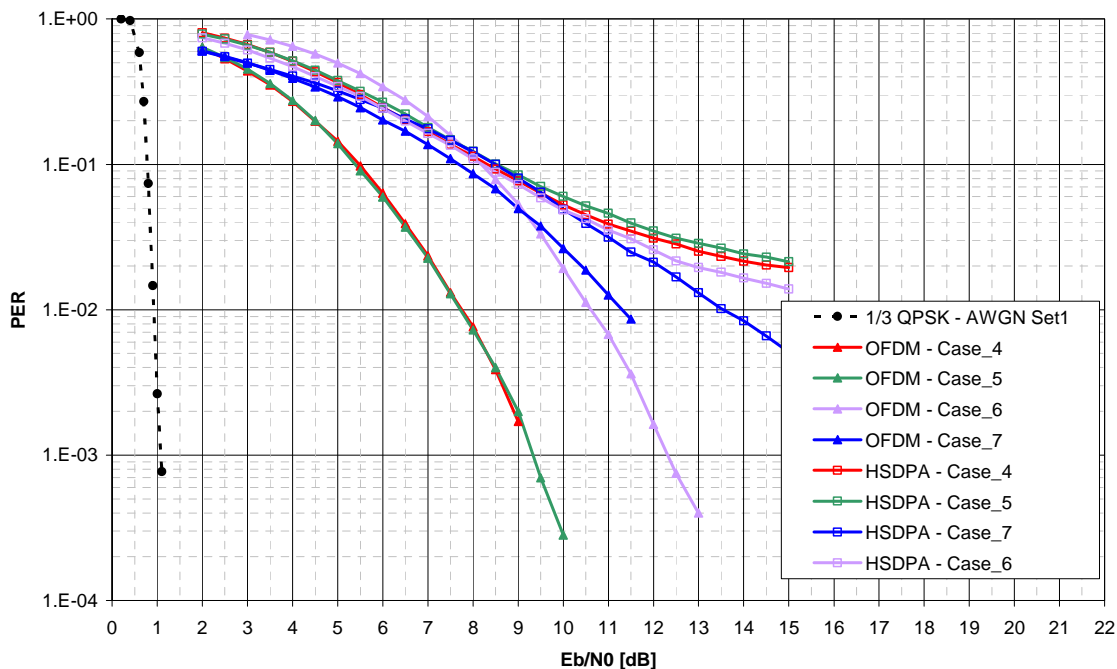


Figure 30: OFDM vs. HSDPA comparison for S-DMB multi-path channels: Case-4, Case-5, Case-6 and Case-7. Terminal speed set to 100 km/h

In figures 29 and 30, the seven S-DMB multi-path channels are simulated assuming a terminal speed equal to 100 km/h. Except for the first two cases, the OFDM results outperform significantly the HSDPA PER performance. In essence, these channel profiles highlight the Rake-receiver incapability to solve the induced multi-path interference emphasized also by the low spreading factor, SF=16. All HSDPA performance shows a PER floor in the order of $2\text{-}3 \times 10^{-2}$, thus a post-equalization process is needed.

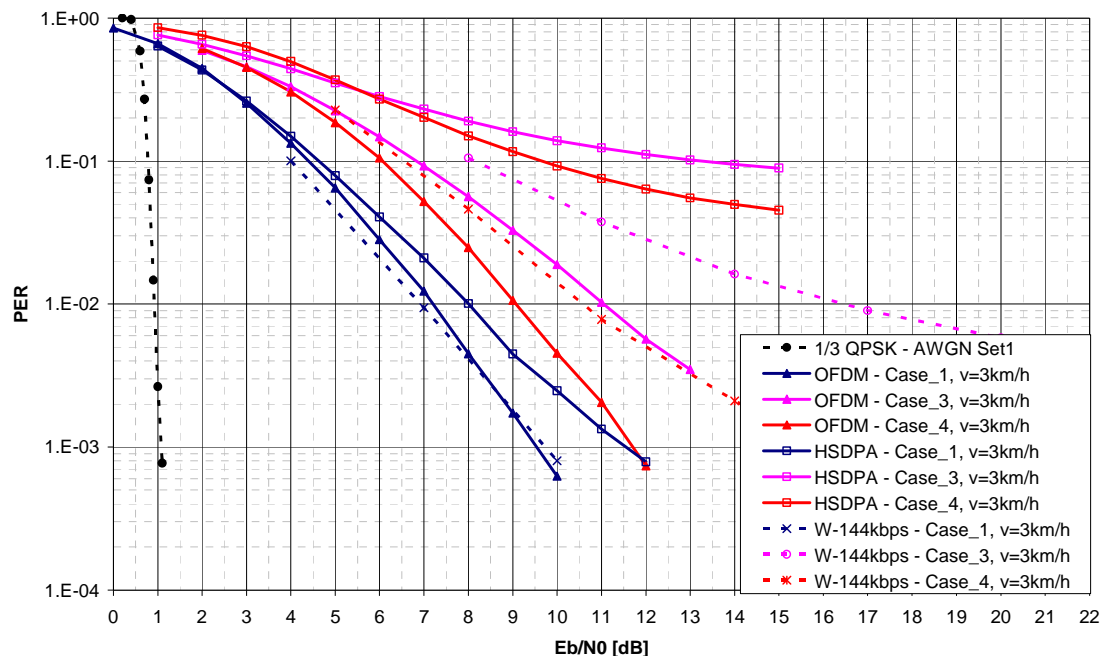


Figure 31: OFDM vs. HSDPA comparison for S-DMB multi-path channels and slow terminal mobility

Figure 31 shows the OFDM and HSDPA comparison for some S-DMB channel profiles decreasing the terminal speed down to 3 km/h. In addition, from the IST MAESTRO project, the WCDMA performance with 144 kbps is reported. Again, OFDM has better performance and, with respect to the WCDMA results, has also increased the system efficiency.

For the sake of completeness, the IBO impact on OFDM performance is reported in figure 32 for a terminal speed equal to 100 km/h and the S-DMB Case-1 multi-path channel. As expected, decreasing the IBO working point the OFDM PER performance improves. In addition, the linearized TWTA model (LTWTA) is introduced and no predistortion techniques are implemented. In this case, the performance between TWTA IBO=2 dB and LTWTA IBO=2 dB is comparable.

Finally, the carrier frequency error is considered in figure 33. It can be noted that the degradation loss is almost negligible for normalized residual frequency errors up to $0,1/N$ (where N is the number of IFFT/FFT points). When an error equal to $0,2/N$ is simulated, the OFDM performance loss is in the order of 1,5 dB at $\text{PER}=10^{-2}$.

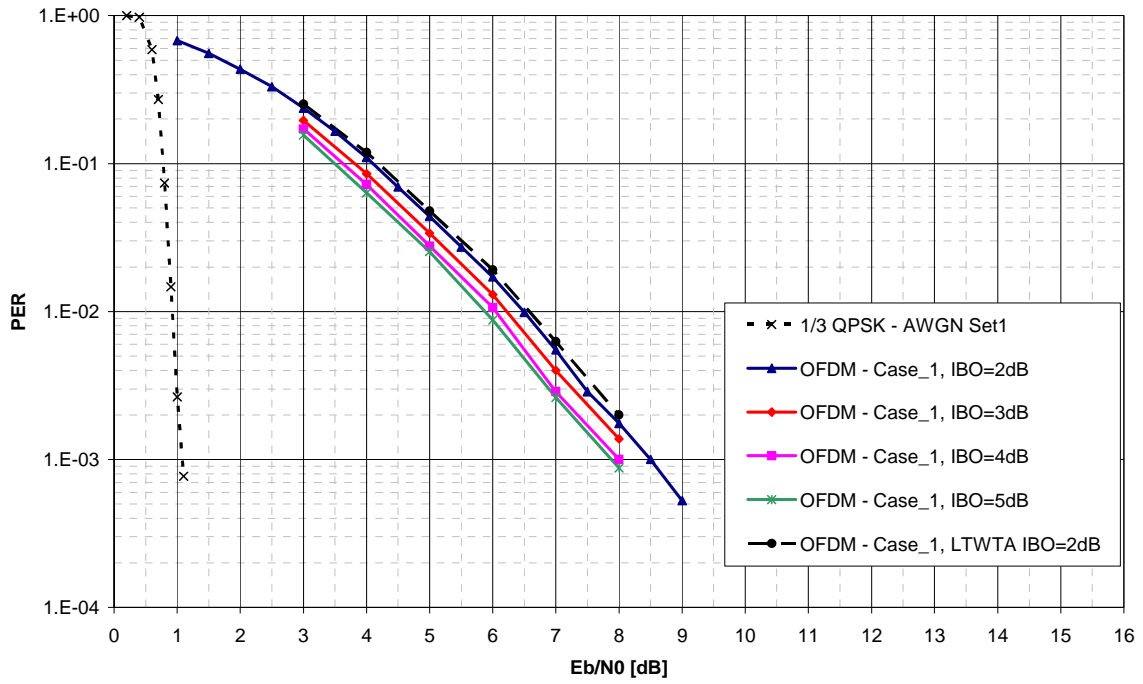


Figure 32: IBO impact on OFDM performance

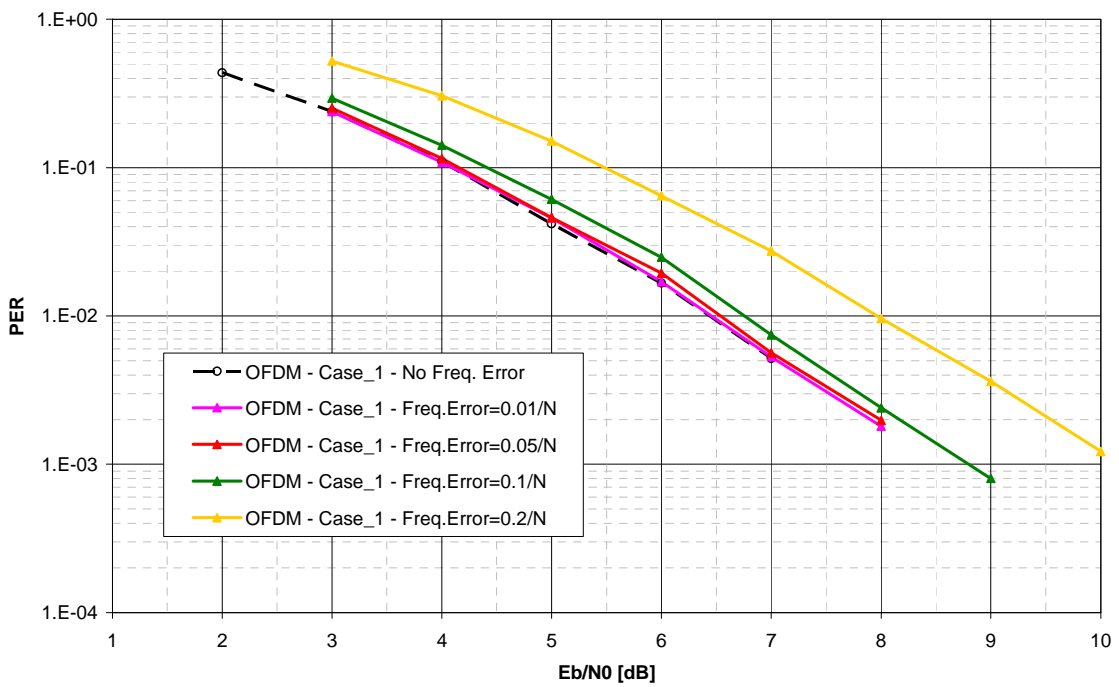


Figure 33: Carrier frequency error impact on OFDM performance

9 Link Budget Study

9.1 System parameters

9.1.1 Satellite parameters

Satellite parameters are summarized in table 11.

Table 11: Satellite parameters

Satellite location	10°E
Useful EIRP for traffic per spot per carrier at EOC	68,5 dBW
Antenna polarization	Circular

9.1.2 UE parameters

Satellite parameters are summarized in table 12.

Table 12: UE parameters

UE type	Handset	Handheld	Vehicular
G/T	-29,1 dB/K	-27 dB/K	-21 dB/K
Polarization losses	3 dB	0 dB	0 dB
UE elevation	35°		

9.1.3 Physical layer configuration and performances

Physical layer configuration and demodulation performances are summarized in table 13. Rx required C/N values are derived from Eb/No values for a PER of 10^{-2} .

Table 13: Physical layer configuration and performances

OFDM parameter set	Set 1
Bandwidth	4,485 MHz
Data rate	2,4 Mbps
Rx required C/N, AWGN, static	-1,7 dB
Rx required C/N, Case 1, 3 km/h	4,5 dB
Rx required C/N, Case 1, 100 km/h	3,8 dB
Rx required C/N, Case 3, 3 km/h	8,3 dB
Rx required C/N, Case 3, 100 km/h	6,3 dB

9.2 Link budgets

9.2.1 Handset

Service reception in Case 3 propagation environment at 3 km/h is not possible for handset due to negative link margin as shown in grey columns in the link budget presented in table 14. Nevertheless this could be counteract by introduction of long term interleaving in MAC layer so that Case 3 at 3 km/h could be operated with secured link margin.

Table 14: Link budget; Handset

		Handset				
		AWGN	Case 1	Case 1	Case 3	Case 3
		Set 1 Static	Set 1 3 km/h	Set 1 100 km/h	Set 1 3 km/h	Set 1 100 km/h
Satellite Parameters						
Satellite Location	°E	10	10	10	10	10
Orbital Height	Km	35 786	35 786	35 786	35 786	35 786
Link Parameters						
Full FDM Bandwidth	MHz	4,485	4,485	4,485	4,485	4,485
Data Rate	kbps	2 400	2 400	2 400	2 400	2 400
Required Rx C/N	dB	-1,7	4,5	3,8	8,3	6,3
UE Location						
Elevation		35,00	35,00	35,00	35,00	35,00
Slant Range	Km	38 180,8	38 180,8	38 180,8	38 180,8	38 180,8
Downlink Frequency	MHz	2 182,5	2 182,5	2 182,5	2 182,5	2 182,5
Availability (/year)	%	99,99	99,99	99,99	99,99	99,99
Polarization (C/V/H)	C/V/H	Circular	Circular	Circular	Circular	Circular
On Board EIRP/Beam / for Traffic	dBW	68,5	68,5	68,5	68,5	68,5
UE G/T	dB/K	-29,1	-29,1	-29,1	-29,1	-29,1
Polarization losses	dB	-3	-3	-3	-3	-3
Losses (free space, rain, atmos.)	dB	190,9	190,9	190,9	190,9	190,9
Total Received PFD	dBW/m ² /1 MHz	-171,4	-171,4	-171,4	-171,4	-171,4
DL C/No	dBHz	74,0	74,0	74,0	74,0	74,0
Link Margin	dB	9,2	3,0	3,7	-0,8	1,2
Power level at UE antenna connector	dBm	-95,4	-95,4	-95,4	-95,4	-95,4

9.2.2 Handheld

Link budget for handheld is presented in table 15.

Table 15: Link budget; Handheld

		Handheld				
		AWGN	Case 1	Case 1	Case 3	Case 3
		Set 1 Static	Set 1 3 km/h	Set 1 100 km/h	Set 1 3 km/h	Set 1 100 km/h
Satellite Parameters						
Satellite Location	°E	10	10	10	10	10
Orbital Height	Km	35 786	35 786	35 786	35 786	35 786
Link Parameters						
Full FDM Bandwidth	MHz	4,485	4,485	4,485	4,485	4,485
Data Rate	kbps	2 400	2 400	2 400	2 400	2 400
Required Rx C/N	dB	-1,7	4,5	3,8	8,3	6,3
UE Location						
Elevation	°	35,00	35,00	35,00	35,00	35,00
Slant Range	Km	38 180,8	38 180,8	38 180,8	38 180,8	38 180,8
Downlink Frequency	MHz	2 182,5	2 182,5	2 182,5	2 182,5	2 182,5
Availability (/year)	%	99,99	99,99	99,99	99,99	99,99
Polarization (C/V/H)	C/V/H	Circular	Circular	Circular	Circular	Circular
On Board EIRP/Beam / for Traffic	dBW	68,5	68,5	68,5	68,5	68,5
UE G/T	dB/K	-27,6	-27,6	-27,6	-27,6	-27,6
Polarization losses	dB	0	0	0	0	0
Losses (free space, rain, atmos.)	dB	190,9	190,9	190,9	190,9	190,9
Total Received PFD	dBW/m ² /1 MHz	-171,4	-171,4	-171,4	-171,4	-171,4
DL C/No	dBHz	78,5	78,5	78,5	78,5	78,5
Link Margin	dB	13,7	7,5	8,2	3,7	5,7
Power level at UE antenna connector	dBm	-91,4	-91,4	-91,4	-91,4	-91,4

9.2.3 Vehicular

Link budget for vehicular is presented in table 16.

Table 16: Link budget; Vehicular

		Vehicular				
		AWGN	Case 1	Case 1	Case 3	Case 3
		Set 1 Static	Set 1 3 km/h	Set 1 100 km/h	Set 1 3 km/h	Set 1 100 km/h
Satellite Parameters						
Satellite Location	°E	10	10	10	10	10
Orbital Height	Km	35 786	35 786	35 786	35 786	35 786
Link Parameters						
Full FDM Bandwidth	MHz	4,485	4,485	4,485	4,485	4,485
Data Rate	kbps	2 400	2 400	2 400	2 400	2 400
Required Rx C/N	dB	-1,7	4,5	3,8	8,3	6,3
UE Location						
Elevation	°	35,00	35,00	35,00	35,00	35,00
Slant Range	Km	38 180,8	38 180,8	38 180,8	38 180,8	38 180,8
Downlink Frequency	MHz	2 182,5	2 182,5	2 182,5	2 182,5	2 182,5
Availability (/year)	%	99,99	99,99	99,99	99,99	99,99
Polarization (C/V/H)	C/V/H	Circular	Circular	Circular	Circular	Circular
On Board EIRP/Beam / for Traffic	dBW	68,5	68,5	68,5	68,5	68,5
UE G/T	dB/K	-21,0	-21,0	-21,0	-21,0	-21,0
Polarization losses	dB	0	0	0	0	0
Losses (free space, rain, atmos.)	dB	190,9	190,9	190,9	190,9	190,9
Total Received PFD	dBW/m ² /1 MHz	-171,4	-171,4	-171,4	-171,4	-171,4
DL C/No	dBHz	85,1	85,1	85,1	85,1	85,1
Link Margin	dB	20,3	14,1	14,8	10,3	12,3
Power level at UE antenna connector	dBm	-88,4	-88,4	-88,4	-88,4	-88,4

10 Conclusions

From the set of results that have been collected in this work item, the following conclusions and indications can be drawn:

- It appears that, notwithstanding the large PAPR, it is possible to efficiently transmit OFDM signals through non-linear satellite links with very small IBO and OBO values.
- This surprising result is the fruit of virtuous cross-fertilization between careful predistortion design and powerful forward error correction coding application.
- In frequency flat correlated Rice fading channels and perfect channel estimation, OFDM produces small losses with respect to the HSDPA interface due to only the guard-time insertion.
- In multi-path channel conditions (satellite and CGC links), OFDM shows its robustness and, for the considered S-DMB channel profiles and with ideal channel estimation, OFDM outperforms the Radio Interfaces based on WCDMA and HSDPA. Notably, this is achieved considering the same spectrum occupancy specifications.

- The link budget study shows that proper service reception can be attained in satellite LOS conditions. In satellite NLOS propagation conditions, proper service reception could not be achieved with this radio interface when considering an handheld terminal, due to a negative link margin. Nevertheless, the use of CGCs can be a viable solution to restore proper service reception in areas where satellite reception is critical.
- Computing the corresponding link budgets for the HSDPA case results in lower margin for all those cases where the required Rx C/N is higher than for the OFDM case and this is especially true in the NLOS case and when CGCs are considered.

History

Document history		
V1.1.1	August 2008	Publication